

Article

Films Floating on Water Surface: Coupled Redox Cycling of Iron Species (Fe(III)/Fe(II)) at Soil/Water and Water/Air Interfaces

Hong Zhang ^{*}, Zac Rush, Zoe Penn, Kami Dunn , Sydney Asmus, Carolyn Cooke, Zach Cord, Shawna Coulter and Chance Morris 

Department of Chemistry, Campus Box 5055, Tennessee Tech University (TTU), Cookeville, TN 38505-0001, USA
* Correspondence: hzhang@tntech.edu

Abstract: Naturally occurring Fe(III) films with rainbow reflection iridescence have been observed floating on the water surface of various spots covered with shallow water (e.g., edges of wetlands and creeks, standing water over soils). This natural phenomenon has become a scenic attraction and stimulated much curiosity. We pursued an experimental inquiry aimed at probing this interesting, curious natural wonder. As the first critical task, floating Fe(III) films were successfully generated in an assessable, controllable setting in our laboratory. This enabled us to establish this phenomenon reproducibly under controlled conditions and characterize the phenomenon over the entire span of the formation and transformation of the Fe(III) films. Our film generation method requires a few things: fresh soil (source for Fe(III) and microbes), glucose (energy source), and water in a container. The floating Fe(III) films as observed in the field occurred in ~1–3 day(s) on the water surface of the inundated soil mixed with the sugar. The Fe(III) films then grew from initial very thin, colorless, somewhat transparent films with rainbow reflection iridescence to colored thicker films and then to orange/orange-red/red crusts over the time. A comprehensive mechanistic picture was formulated to depict the formation of the Fe(III) films. Several sequential processes are operative. First, the Fe(III) (oxides, oxyhydroxides) in the soil is reduced to Fe(II) by the Fe(III)-reducing microbes during their anaerobic respiration with Fe(III) as the electron (e^-) acceptor after depletion of dissolved O_2 in the water as a result of aerobic microbial respiration with O_2 as the e^- acceptor. The Fe(II), being soluble, then diffuses to the water surface where it is oxidized to Fe(III). Subsequently, the Fe(III) hydrolyzes and various Fe(III) hydrolysis products polymerize to stabilize. A polymeric model was created to account for the Fe(III) film transformation. The Fe(III) films are considered to transform from the dimers and trimers and linear polymers of $Fe(OH)_3$ to Fe(III) polymer sheets (e.g., $Fe(OH)_3$, $FeOOH$), to 3D Fe(III) polymers, and eventually to Fe_2O_3 colloid particles. This floating Fe(III) film phenomenon boasts an environmental chemical drama of redox cycling of Fe(III)/Fe(II) at soil/water and water/air interfaces coupled with Fe(II) transport from the inundated soil to the water surface followed by ultimate mineralization of the Fe(III) polymers. Our Fe(III) film generation method can be readily scaled up to supply Fe(III) films of rich varieties in thickness, size, morphology, and structure over the entire span of various stages of their formation and transformation as desired for various uses. This setup offers a platform needed for further controlled studies on the kinetics, mechanism, and process of abiotic and biotic nature involved in the Fe(III) film phenomenon and for exploration of versatile roles of the Fe(III) films as nanofilms in Fe(III)/Fe(II)-surface catalyzed chemical and photochemical reactions involving various natural and synthetic compounds.



Citation: Zhang, H.; Rush, Z.; Penn, Z.; Dunn, K.; Asmus, S.; Cooke, C.; Cord, Z.; Coulter, S.; Morris, C. Films Floating on Water Surface: Coupled Redox Cycling of Iron Species (Fe(III)/Fe(II)) at Soil/Water and Water/Air Interfaces. *Water* **2024**, *16*, 1298. <https://doi.org/10.3390/w16091298>

Academic Editor: Giovanni Esposito

Received: 22 March 2024

Revised: 22 April 2024

Accepted: 23 April 2024

Published: 2 May 2024



Copyright: © 2024 by the authors. Licensee MDPI, Basel, Switzerland. This article is an open access article distributed under the terms and conditions of the Creative Commons Attribution (CC BY) license (<https://creativecommons.org/licenses/by/4.0/>).

Keywords: condensation polymerization; electron acceptor; ferric; ferrihydrite; ferrous; glucose; microbes; nanofilms; oxides; oxyhydroxides; rainbow reflection iridescence; redox boundary; redox interface; wetlands

1. Introduction

Iron is unique and ubiquitous.

With the highest binding energy per nucleon, iron boasts the last chemical element with a stable nucleus (Fe(26)) that is generated in a star during its stellar nuclear fusion [1–4]. It has the highest cosmic abundance among the metal elements [5,6] and is the fourth most abundant element in the Earth's crust [7,8]. As the most abundant element on Earth as a whole (~30% of Earth's total mass) [7], iron is the major chemical component of the Earth's core [5,7,9]. The Fe(III)/Fe(II) couple is considered to be intimately associated with the origin of life [10]. Biological systems have iron as their prominent member [7,11–14]. Hemoglobin, the pivotal blood biomolecule, finds iron occupying its magnificent protein assembly with a vital biochemical role to play [12,15,16].

Iron lends itself to everywhere in the environment. It commonly exists in water, soil, and air [17]. Iron binds humic substances, widely present in soils and waters [18–20]. Iron oxyhydroxides and oxides color soils in a spectrum of orange to red [20,21]. Airborne dusts containing iron originated from the Sahara Desert travel across the ocean, landing on another continent [22]. Oceanic scarcity of iron renders it to become a limiting nutrient for alga in oceans [23]. This oceanic ecological feature of iron inspired a novel attempt to boost oceanic algal bloom by artificial addition of iron to the ocean aimed at CO₂ fixation (oceanic iron fertilization) [17,24].

Playing a pivotal role in environmental chemistry [25,26], iron can control a great number of environmental chemical reactions, especially reduction and oxidation (redox) reactions, and photochemical and surface reactions (e.g., see [26–31]). Iron plays a critical role in biogeochemical cycles of various nutrients and many other elements [26,32,33].

Fe ([Ar]3d⁶4s²) has two stable redox species commonly found in the environments, ferric iron (Fe(III): Fe(Ar)3d⁵) and ferrous iron (Fe(II): Fe(Ar)3d⁶). The Fe(III) species are insoluble, existing as hydroxides (Fe(OH)₃), oxyhydroxides (FeOOH), and oxides (e.g., Fe₂O₃) [11], while Fe(II) is soluble and thus mobile in soils, sediments, and waters. The Fe(III)/Fe(II) redox couple can undergo a redox cycling between Fe(III) and Fe(II):



Iron has a rich repertoire of redox reactions involving the Fe(III)/Fe(II) redox couple and cycling [26,33]. A prominent, important feature of Fe environmental chemistry lies at the coupling of Fe redox cycling with physical transport of Fe in waters and soils as a result of the soluble nature of Fe(II) species and insoluble nature of Fe(III) species.

Fe(II) can be readily oxidized to Fe(III) in soils and waters and then hydrolyze to form Fe(III) hydroxides, which further transform to Fe(III) oxyhydroxides and then oxides [26]. The oxidation of Fe(II) is especially active at redox interfaces such as water/air and soil/air interfaces where exists a redox potential change (redox gradient) [34]. Fe(III) species can be reduced to Fe(II) chemically (photochemical, surface reactions) and biotically (microbially via respiration) in soils and waters [26]. Anaerobes resort to other electron (e^-) acceptors than O₂ (e.g., Fe(III), Mn(IV), NO₃⁻/NO₂⁻, SO₄²⁻, etc.) for their anaerobic respiration [26,35,36] after dissolved oxygen (DO) is depleted [37]. Hence, Fe(III)/Fe(II) redox cycling is coupled not only with Fe transport but also with biotic activities in soils and waters.

Natural phenomenon of floating Fe(III) films and origin of the present study. The natural phenomenon of mysterious films floating on water surface delivers a marvelous highlight of the fascinating environmental redox chemistry of iron (Figure 1). Previously, oil-like floating thin films with rainbow shining were observed appearing on the surface of somewhat shallow water near the edge of a wetland; yet, a finger-poking of the film resulted in breaking of the films, instead of climbing onto one's fingertip (see Figure 1b). This refutes the illusion of oily (hydrophobic) films and in turn suggests the hydrophilic nature of the films (Rich Bartlett, personal communication, 1993 [37–39]). It was thought that the films observed are composed of some forms of Fe(III) hydroxides/oxyhydroxides

associated with microbially mediated redox transformation of Fe(III)/Fe(II) coupled with Fe(II) transport (Rich Bartlett, personal communication, 1993).



(a)



(b)

Figure 1. Iridescent floating films naturally occurring on water at (a) Cane Creek Lake Park (2022, Cookeville, TN, USA) and (b) a wetland (1998, Tahquamenon River Watershed, MI, USA).

One can come across the floating Fe(III) films on a field trip, a leisure walk in a park with shallow streams or waters in sight, or various outdoor settings (Figure 1), and many other places around the world [37,39]. The floating films have also called the attention of a group of keen researchers with acute curiosity that led to investigations into the chemical nature of the films and the processes involved in their formation [37–40].

Yet, the mystery of this fascinating natural phenomenon remains to be fully unveiled. Because where and when the floating Fe(III) films may occur in our natural environments remain largely unpredictable, this phenomenon needs to be repeatably established under controlled conditions and fully characterized for its entire span from intimal thin films to thick films and crusts. Moreover, its complete environmental chemical picture still needs to be revealed. This necessitates full-scale experimental investigations. The research of such a sort calls for certain prerequisites, including (a) a film generation setup (method) that is conveniently operative and experimentally controllable and (b) the Fe(III) films that are repeatably available as desired.

Previously published studies on floating Fe(III) films resorted to the use of naturally occurring [37,39] or laboratory synthetic [39] films or the films formed in enriched media prepared by laboratory incubation of field-collected, selected natural sediment samples [40]. These sources of Fe(III) films bear some limitations. Naturally occurring Fe(III) films collected in the field might not be reproducible in their sampling location (site, spot) and environmental setting, their size, quantity, color, thickness, or structure, their chemical and mineralogical makeup and characteristics, or the stage (phase) of their growth and

aging, which all appear to be more or less at the mercy of chance upon film sampling. The variation and non-reproducibility of film sampling could cast uncertainties on the representativeness of the films used in the previous studies. The synthetic films and those from the selected, incubated sediment media, on the other hand, involved a complicated series of highly technical laboratory operations that require well-trained hands in addition to certain specialty equipment [39,40]. Incidentally, these films thus produced may not necessarily reproducibly resemble naturally occurring Fe(III) films.

The lack of a reproducible, controllable supply of Fe(III) films ready in a laboratory setting challenged further in-depth full-scale controlled investigation. Hence, there is a compelling need to find a method to be able to generate Fe(III) films that is conveniently assessable and readily controllable and can repeatably deliver them. A discovery occurred in our laboratory, namely, that it was accomplishable to generate the Fe(III) films in our laboratory setting as desired [41,42], which then paved the way for a wide scope of novel research to fully establish and characterize this natural phenomenon and to reveal and understand the mechanism and process of the formation and transformation of the Fe(III) films, as described below in the objectives of this research.

Objectives of the present study. The objectives of the present research were to (1) generate naturally occurring floating Fe(III) films in a laboratory setting using a method that can deliver the films repeatably and controllably as desired across the entire span of the formation and transformation of the films; (2) fully establish the floating Fe(III) film phenomenon reproducibly and consistently; (3) characterize this phenomenon over the entire span of its formation and transformation; (4) experimentally investigate the Fe(III) film phenomenon using our film generation setting to understand this phenomenon; (5) formulate a comprehensive mechanistic picture of the Fe(III) film formation in terms of fundamental principles of environmental chemistry and established understanding of iron chemistry and environmental microbiology with fine technical details, especially in connection with the results of our own experimental work; and (6) create a polymeric model to account for the transformation of the Fe(III) films over its entire span. Hence, this research readily paves the way for further multi-faceted studies on the Fe(III) film phenomenon and for exploration of various potential applications of the Fe(III) films as nanofilms. The merit of our method for demonstration and investigation of the floating Fe(III) film phenomenon as a natural wonder may extend to general education in environmental science as well as environmental chemistry. Ample background information and elaborated presentation with technical details are thus provided for a broader range of readers, without the need of immediate access to the original references.

2. Materials and Methods

The laboratory setting and items needed for this research were common, and easily accessible or home-available. These include fresh soil, water, sugar, calcium carbonate, and a container. A pH meter/paper and Fe(II) test kit are needed for further mechanistic investigation. Generally, the occurrence of the floating Fe(III) film phenomenon requires the following necessities and conditions: (1) iron oxides/oxyhydroxides (Fe(III)) in the soil; (2) fresh, living functional microbes in the soil; (3) mild pH condition (~6–8) and favorable nutritional condition for microbes to flourish to reduce Fe(III) to Fe(II); and (4) inundation of the soil sample in the container (soil sample covered with shallow water) to facilitate the creation of an anoxic (anaerobic, reducing) condition in the submerged soil system.

2.1. Soils

To identify the soil samples needed to replicate the floating Fe(III) film phenomenon in a laboratory setting, fresh soil samples were collected in the field from a variety of places around the city of Cookeville (TN, USA) (Table 1). The samples collected were labeled and sealed in plastic bags and stored in a refrigerator (to keep them fresh) for further use.

Table 1. Summary of the soil samples collected around Cookeville (TN, USA) and the results of the general demonstration tests (Expt.–1) for the floating Fe(III) film phenomenon.

Test	Soil Sample	Location	Site	Test Result
Positive Result ¹	P1	Cummins Falls	Near a creek	Thick crust, red, fastest
	R2	Lafayette	Turtle pond	Thin film, iridescent
	R3	Lafayette	North of back pond	Thin film, small patches, no color
	R4	Lafayette	Stream cross-section	Thick crust, red, slowest
Negative Result ²	P2	Cummins Falls	Next to a wheat field	No film
	R1	Lafayette	Cow prints in main creek	No film

Note: ¹ Positive: films present. ² Negative: films absent.

Fresh soil samples. In order to replicate the floating Fe(III) film phenomenon, fresh soil samples collected in the field must be used. The requirement of fresh field soils stems from the need for fresh, living functional soil microbes co-existing in the soils. At present, it remains rather unclear exactly which groups of soil microbes are specifically responsible for the occurrence of floating Fe(III) films in a particular soil. Hence, the knowledge of which soil would carry and house the required soil microbes apparently appears to be in the hands of luck when a soil sample is taken. As a result, it could happen that some soil samples may not necessarily deliver the desired floating film phenomenon. Nevertheless, our experiences indicate that the required soils are widely and readily available in the field because the functional microbes are commonly present in soils.

Soil iron oxides and oxyhydroxides. Another indispensable component required for the occurrence of floating Fe(III) films is iron oxides and/or oxyhydroxides (as Fe(III) sources) present in soils. The best candidates for soils to be used are those with orange-to-red colors (or some parts of the soils with these colors), which are typical of and thus indicative of the presence of iron oxides/oxyhydroxides in the soils.

The requirement of soil iron oxides/oxyhydroxides suggests that the soils in the southern regions (humid, warm or hot; subtropical or tropical) may be favorable, with a higher chance for the films to occur because these soils commonly have plenty of iron oxides/oxyhydroxides, as shown by their soil color (red soils). Some layers (horizons) of soils in the northern regions may also have adequate iron oxides/oxyhydroxides. If a soil has few iron oxides/oxyhydroxides, as a remedy, some can be artificially added to the soil sample, followed by sufficient mixing. This may create an artificial simulation soil sample to test the film phenomenon (provided the soil sample has the required microbes and soil conditions).

The absence of visible orange-to-red colors in a soil does not necessarily lead to a ruling that the soil does not have iron oxides/oxyhydroxides. It could happen that the soil particles with iron oxides/oxyhydroxides may be covered (coated or wrapped) by organic matter (dark color), which thus can mask the colors of iron oxides/oxyhydroxides.

Soil sampling location and site (spot). The location and site of soil sampling are non-specific because, generally, the components required for the natural phenomenon of floating Fe(III) films to occur are widely present in soils. The specific spot in a soil profile for soil sample collection is not crucial. Any spot (site and location as well) of interest would warrant a collection. Except for the rule-of-thumb feature of orange-to-red colors to serve as a practical marker indicating the presence of iron oxides and/or oxyhydroxides in the soils, soil sampling in terms of geographical location and sampling site or spot can be quite arbitrary as desired. In other words, for the purpose of soil sampling to showcase the floating Fe(III) film phenomenon, the soils needed are not site-specific or spot-specific. Generally, the floating Fe(III) film phenomenon should be expected to occur in a wide range of samples among various soils collected from various places and spots.

Our experiences suggest that the soil samples that failed to deliver floating Fe(III) films may not possess the functional soil microbes, Fe(III) oxides and/or oxyhydroxides,

or favorable soil conditions, in part or collectively, required for film occurrence. Freshly collected soil samples may be stored in a refrigerator for a prolonged period of time and the soil microbes seem to be able to sustain long-term survival in storage.

2.2. Chemicals

The chemicals needed for the present study are described below.

Glucose ($C_6H_{12}O_6$): The sugar is added to boost the flourishing of soil microbes. The rationale for this procedure is that the organic matter originally present in a soil may not provide adequate microbial food (favorable, ready to be consumed) required to induce and sustain the flourishing growth of a variety of functional soil microbes on the scale required for full film occurrence. If glucose is not available, any common sugar should do.

Glucose is preferred since it is the simplest sugar (monosaccharide) that can serve as easy, fast food for the soil microbes to consume without need for initial digestion. This is why the soil organic matter present in a soil is usually not favored or useful, since it entails abundant metabolic activities to transform the organic substances (even the well-defined carbohydrates, fatty acids, and fats) first to the simplest sugars, ready for direct microbial use. Soil organic matter (mainly humic substances) bears a rich variety of (fused) aromatic compounds that can be highly resistant to microbial (enzymatic) attack. The soil organic matter may sustain the minimal survival of the soil microbes and other ordinary ecological activities, but it does not jump-start microbial flourishing in a manner that can quickly deliver a typical floating film occurrence.

Our research indicates that adding sugar turns out to be a critical measure; addition of sugar is responsible for jump-starting the soil microbial activities needed for the floating Fe(III) film phenomenon to occur. This is why the floating film may not commonly materialize readily in a setting only with a fresh field soil sample submerged in water.

Calcium Carbonate ($CaCO_3$): The limestone chemical is used to modify soil pH to provide a mild system condition favored for microbial growth and film formation (pH: ~6–8 generally). Addition of calcium carbonate is especially beneficial for soils in the southern regions, which are commonly acidic (acidic soils or acid soils).

Water: Distilled water is sufficient. Other types of water can work as well. The type of water is not crucial (as long as the water used is clean).

Nitrogen (N_2) gas: This was used to degas dissolved oxygen or expel oxygen in the headspace to create an anaerobic condition in the system tested.

Ferrous Ammonium Sulfate ($Fe(NH_4)_2(SO_4)_2 \cdot 6H_2O$, Baker, ACS Reagent): The ferrous salt was employed to artificially, abiotically generate floating Fe(III) films in a laboratory setting. Ferrous nitrate is not favorable because nitrate (i.e., NO_3^-) can be photochemically sensitive (a source of $\cdot OH$ free radical in irradiated water) and induce photochemically mediated redox transformations involving Fe(III)/Fe(II).

It needs to be pointed out that throughout the present research, neither grade nor accuracy of quantification (weighing) of the above chemicals is critical.

2.3. Materials

The major material for generating floating Fe(III) films in a laboratory setting is a container with a size as desired. The container can be a glass beaker, a paper cup for drinks, a plastic food bowl, or a plastic box or tray. Our research shows that all containers can work just fine. The soil microbes seemed to feel at home in various containers.

2.4. Experimental Studies and Procedures

We conducted three sets of experimental work to create, demonstrate, and investigate the floating Fe(III) film phenomenon in a laboratory setting: (1) creation and general demonstration of the floating Fe(III) film phenomenon using various soils, (2) full-scale case study/demonstration and investigation of the Fe(III) film phenomenon, and (3) a set of experimental tests to probe and understand the process and mechanism involved in the

Fe(III) film phenomenon. The experimental procedures and operational details for each particular set of the work are described below.

General experimental setup and procedures: To generate floating Fe(III) films in our laboratory setting, we prepared a mixture of (1) a fresh soil sample with (2) glucose (i.e., $C_6(H_2O)_6$) powder, (3) calcium carbonate ($CaCO_3$) powder (a natural, mild chemical used to mediate the pH), and (4) deionized water (DI- H_2O) in a small beaker (Don Ross, Soil Redox Laboratory for Soil Chemistry), as these are favorable for microbial growth and mediation. Glucose provides fast food (easily accessible energy source) for soil microbes to engage in their biotic activities, while limestone and water help to nurture the mild soil pH condition needed for the microbes to flourish in a moist environment.

The field-collected fresh, moist soil samples (or stored in plastic bags in a refrigerator at $\sim 4^\circ$, above freezing point) were used directly as they were, without any pretreatment needed (e.g., no need for grinding, selection, drying, or homogenizing). The exact amount of a soil sample used is not critical, as the soil microbes will grow to the level required for film generation under favorable conditions, even though the number of soil microbes or communities may not be identical from one soil sample to another at the beginning. The quantity of each of the other components needed (i.e., glucose, $CaCO_3$, water) is not critical either and can be scaled up proportionally to the desired level.

After the three components (soil, glucose, and $CaCO_3$) were placed in a container and sufficiently mixed, water was then gently added along the wall of the container until ~ 2 – 3 cm above the soil surface. If the mixing is performed after water is added, the solution above the soil may stay murky as a result of the soil particle suspension caused by mixing.

The size and shape of the container(s) are not critical. But, no matter what container is used, it is critical to ensure that the water level is ~ 2 – 3 cm above the soil surface for the specific treatment described (Table 2). Sufficient water height above the soil is important because it can secure an inundation condition with sufficient water coverage depth needed for dissolved oxygen control in the soil–water mixture.

Table 2. Experimental setup and treatments for Expt.–1 and Expt.–2.

Test	Treatment					
	Soil	Glucose (g)	$CaCO_3$ (g)	DI- H_2O	Container	Other
Expt.–1	P1, P2, R1, R2, R3, R4, 10 g	0.09	0.02	~ 40 mL, or water depth: ~ 2.5 – 3 cm	100 mL glass beaker	Beaker kept open
Expt.–2	R4, ~ 140 g	1.3	0.28	Water depth: ~ 2.5 – 3 cm	Plastic tray $12.8 \times 10.5 \times 4.3$ cm ³	Tray kept open

The submerged soil mixed with glucose and $CaCO_3$ in the container was then left in open air without the need for special attention. The conditions thus set in the soil–water system in the container then triggered the processes. Floating Fe(III) films were expected to emerge gradually in ~ 24 – 48 h and keep evolving over time, depending on the particular soil sample in place. Some water was refilled as needed (along the container wall to avoid disturbing the solution as much as possible) occasionally to maintain the required water level.

Creation and demonstration of the floating Fe(III) film phenomenon in a laboratory setting (Expt.–1, General Demo): We used six fresh soil samples field-collected in Cookeville (TN, USA) (Table 1) to identify those that are able to deliver floating Fe(III) films in a laboratory setting and to generally demonstrate the floating film phenomenon. The specific treatments for Expt.–1 are detailed in Table 2. The setups were prepared as described previously (see *General experimental setup and procedures*) and left alone at room temperature so that the films could generate (water was refilled to maintain its level). We also used disposable cups to explore the possibility of their use in place of glass beakers for future tests and found that the alternative containers served just as well.

Full-scale case study demonstration and investigation of the floating Fe(III) film phenomenon (Expt.–2, Primary Demo/Case Study): We selected one representative soil (R4, Table 1) with a typical film generation outcome based on the results from Expt.–1 and used a plastic tray (a larger container with a greater surface area than the small beakers) and identical procedures as for Expt.–1 to deliver full-scale, detailed demonstration and documentation of the floating Fe(III) film phenomenon. All the required components were employed at the proportionally scaled-up levels (Table 2, Expt.–2). We also conducted a set of tests to reveal the floating Fe(III) film phenomenon.

Experimental tests to probe the process and mechanism of the floating Fe(III) film phenomenon (Expt.–3, Process/Mechanism Study): We investigated the role of glucose, CaCO₃, O₂, and water (quantity, depth) in floating Fe(III) film generation to elucidate the environmental chemical and biological processes behind the floating film phenomenon. The same experimental setup and procedures were adopted as in Expt.–1, except that in some tests, glucose or CaCO₃ was omitted, the water amount (level) was altered, the beaker headspace was first purged with N₂ to remove O₂, or the beakers were covered to cut O₂ supply from the air (Table 3). Again, the R4 soil that delivered the typical floating Fe(III) film phenomenon was selected as the representative soil for all the tests in Expt.–3, Process/Mechanism Study (Table 3). Each test was accompanied by a control test without any treatment.

Table 3. Experimental setup and treatments for Expt.–3 conducted in small beakers.

Test	Soil	Glucose (g)	Treatment		
			CaCO ₃ (g)	H ₂ O Depth (cm)	Beaker Cover
Control	R4	0.09	0.02	2.5	no
Glucose	R4	no	0.02	2.5	no
CaCO ₃	R4	0.09	no	2.5	no
H ₂ O	R4	0.09	0.02	1.5, 2.5, 4	no
O ₂	R4	0.09	0.02	2.5	yes

Monitoring of Fe(II) in the solution during Fe(III) film formation: During the last set of the experiment for Expt.–2, Primary Demo/Case Study, the solution above the soil in the large tray was sampled periodically to analyze Fe(II) and monitor its level variation. For this work, ~2 mL of the solution beneath the Fe(III) film was taken using a plastic dropper each time and placed in a 1 cm cuvette and then 5 drops of 10 mM 2,2'-Dipyridyl solution was added to generate an Fe(II) complex for spectrophotometric analysis. It can occur that sampling Fe(II) in the solution may result in Fe(III) film breakage. However, we observed that new, fresh films emerged later, restoring film coverage on the water surface at the spot disturbed.

Experimental work to create Fe(III) films artificially and abiotically: To further test the mechanistic picture of the floating Fe(III) film phenomenon we proposed, efforts were made to artificially create floating Fe(III) films abiotically so as to simulate the natural floating film phenomenon in a laboratory setting. To this end, we used a ferrous salt (Fe(NH₄)₂(SO₄)₂·6H₂O) to perform simulation experiments to induce abiotic generation of floating films using a setup that mimics the systems where biotically mediated formation of the films occurred in a laboratory setting (i.e., inundated fresh soil in a 100 mL glass beaker). The simulations were carried out by using a mixture of the Fe(II) salt and sand particles inundated with DI-H₂O in a 100 mL glass beaker. Three sets of simulation tests (Simulations I, II, and III) were conducted.

For Simulation I (S1), a mixture of the Fe(II) salt and sand was added to deoxygenated H₂O (by purging the water with N₂ to remove O₂) in a 100 mL beaker, and an additional portion of sand was poured to top the inundated mixture off. The beaker was sealed or kept open to air and then left at room temperature for observation of film generation (see Table 4 for S1 treatments). For Simulation II (S2) and Simulation III (S3) with control tests,

similar procedures to those used for Simulation I were adopted, with some variations (see Tables 5 and 6 for S2 and S3 treatments, respectively).

Table 4. Experimental treatments for Simulation I (S1) for the abiotic generation of Fe(III) films.

Test	Fe(II) Salt (g)	Sand (g)	DI-Water (mL)	N ₂ Purging of Water	Beaker Cover
S1-KS1	0.67	10.9 + 11.5	60	Yes	Yes
S1-KS2	0.67	9.9 + 11.6	60	Yes	No
S1-KS4	0.71	9.4 + 10.5	40	Yes	Yes
S1-GC5	0.65	2 sets *	to 45 mL mark	No	No

Note: * One portion of sand added to 10 mL mark of the beaker, followed by additional layer of sand to 20 mL mark with water added to 45 mL mark.

Table 5. Experimental treatments for Simulation II (S2) * for the abiotic generation of Fe(III) films.

Test	Fe(II) Salt (g)	Sand (g)	DI-Water (mL)	N ₂ Purging of Water	Beaker Cover
S2-KS3	0.77	11.0	60	Yes	Yes
S2-GZ6	~1.8	~5.3	40	Yes	Yes
S2-GZ7	~1.8	~5.3	40	Yes	No
S2-GZ8	~1.8	~5.3	40	No	Yes
S2-GZ9	~1.8	~5.3	40	No	No

Note: * A mixture of the Fe(II) salt and sand was added to the beaker without an additional portion of sand, and water or deoxygenated water was added to the mixture with the beaker covered or left open.

Table 6. Experimental treatments for Simulation III (S3) and the control tests (CT) * for the abiotic generation of Fe(III) films.

Test	Fe(II) Salt (g)	Sand (g)	DI-Water (mL)	N ₂ Purging of Water	Beaker Cover
S3-GC10	0.65	No	50	Yes	Yes
S3-GC11	0.65	No	45	No	No
CT-GZ1	no	5.3	40	No	No
CT-GZ2	no	5.3	40	Yes	No

Note: * A special simulation was carried out in the absence of any sand by adding Fe(II) salt to regular or deoxygenated DI-H₂O with the beaker covered or uncovered. The control tests were performed in the absence of Fe(II) salt with sand only.

2.5. Experimental Measurements

pH measurement: pH was measured using a Mettler Toledo SevenEasy pH meter.

Spectrophotometric analysis of ferrous Fe (Fe(II)): Fe(II) generated in the tests was analyzed spectrophotometrically (Thermo Scientific Genesys 20 spectrophotometer, Thermo Electron Corporation, Madison, WI, USA) using 2,2'-Dipyridyl to form a pinkish-red Fe(II) coordination compound. Calibration was performed using a working Fe(II) standard series of 25, 50, 75, and 100 µM made by using a 100 µM Fe(II) standard stock solution (prepared by adding 0.05 mL (or one drop) of a standard stock solution of 50 mM FeCl₃ in 0.8 M HCl to 25 mL DI-H₂O (or distilled water) with 0.05 mL (or one drop) of 1.5 M NH₂OH·HCl added to the water first).

The working Fe(II) standard solution series (25, 50, 75, and 100 µM) can be obtained by adding, to a 1 cm plastic cuvette, 0.5, 1.0, 1.5, and 2.0 of 100 µM Fe(II) stock solution plus 1.5, 1.0, 0.5, and 0.0 mL of H₂O, respectively, to yield a total of 2.0 mL of one particular working Fe(II) standard solution in the cuvette. Then, 2 mL of water was added to a 1 cm cuvette to prepare the blank solution for the spectrophotometric analysis.

Then, to each of the working Fe(II) standard solutions and also the blank solution prepared in the cuvettes, or a sample solution placed in the cuvette, 5 drops (i.e., 0.25 mL) of the coloring agent solution (10 mM 2,2'-Dipyridyl solution prepared using Vermont Buffer (made of 71.6 mL 100% glacial acetic acid and 40.7 mL 29.5% ammonia, NH₄OH)) was added. After 10 min, after complete formation of the pink-reddish Fe(II)-Dipyridyl complexes in the cuvettes, the absorbance was taken at 522 nm using the blank made [29].

Alternatively, 1,10-phenanthroline can be used to analyze Fe(II) spectrophotometrically after complete formation of orange-red Fe(II) complexes.

Measurement of floating Fe(III) film color: The colors of the floating Fe(III) films were measured using the *Munsell Soil Color Book*. A small piece of the Fe(III) film was collected using a flat-tip stick (or any appropriate tool) and the color of the fresh film sample was immediately compared with a matching color in the *Munsell Soil Color Book* to determine the color code for the film collected (the book provides instructions on its use as well as the color coding system). A delayed color measurement after the film is taken from the solution may give rise to a false color determination as a result of the drying of the film.

Collecting a film sample can disturb or break the films already formed and leave a small hole or an opening, where new films emerged. This observation led to the discovery of a way to obtain fresh, new films. Hence, clearing the water surface from film occupation can leave an opening for fresh, new films to form. By means of this technique, films in various formation and growth stages may be generated and harvested for further use as desired.

3. Results and Discussion

Our research encompasses three major sets of experimental work: (1) the creation and demonstration of floating Fe(III) films in a laboratory setting so as to fully establish this phenomenon and create a method for film generation in a laboratory setting, (2) a full-scale case study of the floating film phenomenon in a laboratory setting to characterize the entire span of film formation and transformation, and (3) an experimental investigation into the mechanistic processes of the phenomenon. The benefit of the first set of work is twofold: first, it accomplished the creation of a film generation method in a laboratory setting; second, it resulted in the emergence and selection of the tested soil, delivering a typical case of the floating film phenomenon for further use in the following two sets of the research.

The floating Fe(III) film phenomenon can be viewed from the perspective of two chronological stages: (1) formation of initial Fe(III) films and (2) transformation of the Fe(III) films. Accordingly, we first formulated a comprehensive mechanistic picture of the Fe(III) film formation followed by a presentation of our experimental work to probe its mechanism and process. Next, we created a polymeric model to depict and understand the transformation of the Fe(III) films followed by a discussing of the film formation and transformation in real environments.

3.1. Creation and Demonstration of the Floating Fe(III) film Phenomenon in a Laboratory Setting

Four (P1, R2, R3, and R4) out of the six tested soils (Table 1) delivered the floating Fe(III) film phenomenon (Figure 2) over a span of ~1–3 days or longer, depending on the soil sample used. This demonstrates our success in creating the natural floating Fe(III) film phenomenon in a laboratory setting. This further indicates that this film phenomenon can occur readily and widely. Our findings point to the notion that the floating Fe(III) film occurrence is indeed a natural phenomenon that involves certain chemical and biological processes orchestrated by a group of natural components in the environment. The results of Expt.-1, General Demo demonstrate that the natural floating Fe(III) film phenomenon observed in the field can be readily generated in a laboratory setting using fresh soils. It then follows that instead of observing it in the field, we can now study this phenomenon in a controllable laboratory setting, which paves the way for various further studies.



(a)



(b)

Figure 2. Examples of the Fe(III) film occurrence on water surface of submerged soils in small glass beakers in a laboratory setting for (a) three tested soil samples, P1, R2, and R4 (Table 1), and (b) an amplified image of the R4 soil with reflective rainbow iridescence and fractal film morphology.

The lack of film occurrence for two of the soils tested (R1 and P2) (Table 1) suggests that there are certain conditions required for the films to materialize. Since all the soils tested received identical treatment, the absence of Fe(III) film in these two soils was likely due to an absence of the required microbial communities and/or their favorable niche. This absence could also stem from a lack of Fe(III) species in the soils tested. If this would be the case, artificially adding Fe(III) oxides/oxyhydroxides to the soil(s) may offer a remedy, especially in the case of northern region soils, which usually possess less Fe(III) oxides and oxyhydroxides than those of southern regions.

The thickness, size, morphology, color, and reflecting iridescence of these films and the speed of their development contribute to their most important physical features. If thin and uniform, they are referred to as films, and if dry and cracked, they are referred to as crusts. The film's color is represented either by iridescence, which means the oil-like coloration in the initial and early stages of formation, or by the color that it produces in

later stages. The color of the films and crusts offers a reflection of the chemical makeup of the Fe(III) species and the stage of development, as discussed in subsequent sections.

In the early stages of formation and growth, the films (Figure 2) were thin, colorless with reflective rainbow iridescence, and in separate small patches with various fractal morphologies (Figure 2). The individual patches eventually fused together to a single piece of apparently uniform thin film, as displayed in the subsequent section.

3.2. Full-Scale Case Study and Characterization of the Floating Fe(III) Film Phenomenon

After the proper soils were first identified for delivery of the films, an amplified demonstration was performed to showcase the phenomenon on a larger scale, followed by a detailed case study to further investigate the Fe(III) film phenomenon. This study was implemented by setting a large plastic tray with all the required components in place at proportionally scaled up levels (Table 2).

Clearly, the Fe(III) film generation in the large tray started with individual, separate small patches of floating, colorless (or somewhat blue reflection) thin films with reflective rainbow iridescence (Figure 3a) and continued to grow and change gradually to thicker films (Figure 3b) and orange/red crusts (Figure 3c) thicker than the initial thin films over a span of ~2 weeks (Table 7, First Test of Case Study).

Table 7. The results of Expt.-2, Primary Demo/Case Study (First Test of Case Study, 2022) with a detailed documentation of Fe(III) film generation and growth in a large tray.

Soil	February 17, 2022	February 18	February 23	March 4, 2022
R4 in tray	Thin films, blue colored	Thin films, iridescent	Thick crusts, orange colored	Thicker crusts, red and orange colored

Shortly after water was added to the setup, a large amount of bubbles appeared in the tray, accompanied by a strong odor typical of anaerobic activities, which indicated strong microbial activities in the tray. The bubbles carried some Fe(II) and some bubbles soon turned orange, as can be seen on the left side/edge of the solution in the tray (Figure 3a), thus indicating oxidation of the Fe(II) present in the bubbles.



(a)

Figure 3. Cont.



(b)



(c)

Figure 3. Primary demonstration of the floating Fe(III) films (Expt.–2, Primary Demo/Case Study) at water surface of the inundated soil (R4) in a large tray (Table 2) for the First Test of Case Study (February–April 2022) as (a) initial thin films in the early stage of the film formation, (b) separate, small patches of films with pronounced rainbow reflection iridescence in the intermediate stage, and (c) orange/red colored crusts in the later stage of film development.

The occurrence of typical floating Fe(III) films in the large tray on an amplified scale (Figure 3, Table 7) not only offers a solid confirmation of the observations and results gained in Expt.–1, General Demo, but also points to a convenient, accessible way in which the floating Fe(III) films can be generated and readily collected at will in larger quantities across various stages of film formation with respect to various physical features (e.g., size, thickness, color, etc.). It follows that this film generation setup and its modification and adaptation can provide a satisfactory, useful means to manufacture the floating Fe(III) films in a laboratory setting.

It was curious how robust and reproducible this large tray setup could be for film manufacture. To explore the capability and potential of our film generation setup, we left the films together with the soil to dry up after the First Test of Case Study was conducted in February–March of 2022 (Figure 3, Table 7) with the tray unattended ever since, and then in early April of 2023 (one year later), we initiated a renewed, identical film test in the same tray from the first test (Figure 3, First Test of Case Study) by freshly adding 1.3 g of glucose (same amount as in the first test shown in Table 2) and required amount of water

(Table 2) to the same water level. Amazingly, an identical recurrence of floating Fe(III) films materialized, as shown in Figure 4 and Table 8 (Second Test of Case Study) in the same manner as in the first test in February–March of 2022 (Figure 3 for First Test of Case Study).

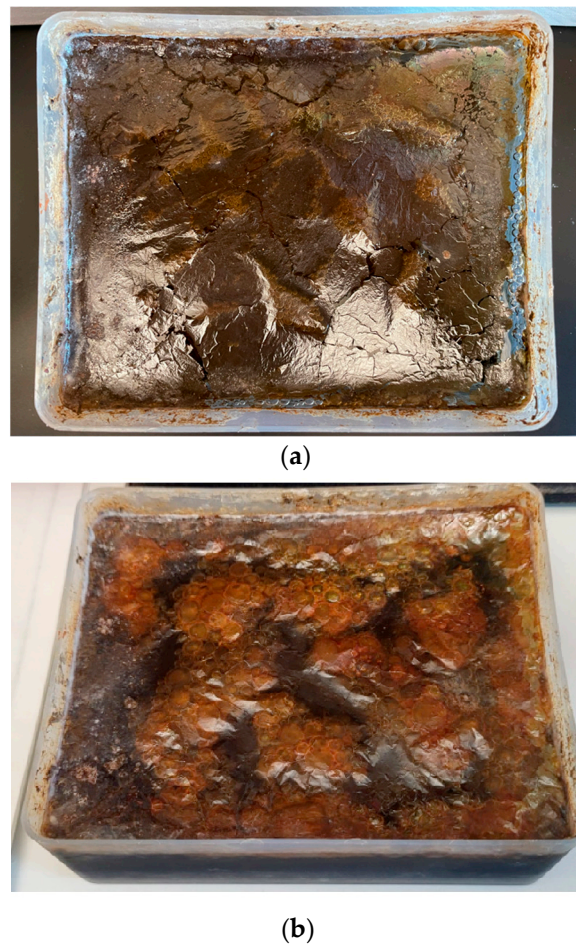


Figure 4. Primary demonstration of the floating Fe(III) films (Expt.–2, Primary Demo/Case Study) at water surface of the inundated soil (R4) in a large tray (Table 2) for the Second Test of Case Study (April–May 2023) (a) on 19 April 2023, ~two weeks after the second test was started for the film formation, and (b) on 27 April 2023, ~three weeks after the second test was started.

Table 8. The results of Expt.–2, Primary Demo/Case Study (Second Test of Case Study, 2023) with a detailed documentation of the reoccurring floating Fe(III) film generation and growth in the large tray.

Date *	April 4	5	6	8	9	11	12	13	14	18	19	April 21
Bubble	Many, small	Full cover	Some, orange	Less	---	---	---	---	---	Small ones	Small ones	Small ones
Odor	Some	Strong	Strong	Less	---	---	---	---	---	---	Some	Less
Film	No	Thin, small patches	Thin, large patches	More films, thicker	More films, thicker	Crust seen	Crust hardened	Thicker crusts				
Film Color	N/A	Colorless	No color	Turning orange	7.5YR/5/8	2.5YR/3/6	---	2.5YR/8/3	2.5YR/8/6	---	---	---
pH	---	---	---	6.3	6.6	---	---	---	---	---	---	---
Fe(II) **	---	A little	Yes	Yes	Yes	Yes	Yes	Yes	Yes	Yes	Yes	Yes

Note: * All the dates are in April of 2023. ** Fe(II): Detailed Fe(II) monitoring results are available in a subsequent section.

The First and Second Tests of Case Study with intermittent drying up of the films and soil delivered the same recurring floating Fe(III) film phenomenon in the same tray and setting. It appears that drying failed to eliminate or compromise the microbes in the soil and they survived the drying; once moisture was restored, the functions and activities of the soil microbes were switched on, which delivered the Fe(III) film phenomenon again.

Out of curiosity, after the First (February–March 2022) and Second (April–May 2023) Tests of Case Study, we again tested the same R4 soil in the original tray with the same setup following the same procedures three more times in 2023. Remarkably, the floating films reoccurred three times in a roll during August–November of 2023, each time in the same expected manner as described previously and shown in Figures 3 and 4 and Tables 7 and 8.

During drying, the Fe(III) films dropped to the dried soil surface. After a restoring of moisture (water added) and under the required conditions, the Fe(III) species in the films resting on the soil surface returned to the water surface (see Figure 4), closing a coupled cycling of Fe(III)/Fe(II) redox transformation with the Fe(III)/Fe(II) transport in the system in the tray (to be elaborated later in technical details). This reoccurring coupled cycling of the Fe(III)/Fe(II) redox and Fe(III)/Fe(II) transport mediated by the soil microbes provides a fine device for renewable manufacturing of the Fe(III) films, available for film harvest in various stages of formation and growth as desired.

During the Second Test of Case Study for the Fe(III) film phenomenon in April–May of 2023, several measurements were conducted to investigate the film phenomenon using the tray setting, which successfully provided a platform for this study. We measured the pH of the solution and the colors of the films in various stages of their development. Moreover, we monitored the Fe(II) level in the solution during film development.

Our measurement showed that the pH of the tested solution beneath the films was ~6–7 (Table 8) right in the circumneutral range, which is a favorable pH condition for soil microbes and Fe(II) oxidation. The pH measurement was discontinued because when the pH probe was inserted into the solution in the tray with the Fe(III) films covering or almost sealing the water surface in some cases, some Fe(III) film patches were stuck to the glass membrane of the pH probe bulb. The Fe(III) film patches can become strongly attached to the glass membrane and thus could potentially cause malfunction of the pH electrode. Hence, care needs to be taken when a pH measurement is made under such circumstances. The pH may also be measured by using a piece of pH paper.

The colors of the films in various stages of development are given in Table 8. The film color changed from initially being colorless (or blue with reflective rainbow iridescence) to orange to orange-red to red. These results suggest that the chemical makeup of the Fe(III) films was evolving with continuous speciation change. Our Fe(II) monitoring test showed that Fe(II) was present at quite high levels with some mild variation, which was sustained during the entire test. The results of the Fe(II) test will be presented in detail in a subsequent section.

The experimental work of Expt.–1 and Expt.–2, conducted in a laboratory setting, demonstrates that the floating Fe(III) film phenomenon is indeed a reproducible, well-established natural phenomenon. This work also successfully provides a characterization of the Fe(III) film phenomenon over the entire span of its formation and transformation from initially thin films to subsequently thicker films and crusts. These research outcomes would be challenging to achieve by in situ observation.

3.3. Floating Fe(III) Film Formation: A Mechanistic Picture

The occurrence of floating Fe(III) films in a laboratory setting as well as that observed in the field stands as a well-established natural phenomenon. This certainly invites an inclination to find out the mechanism behind this natural wonder. This environmental chemical drama, generally, has been considered to involve coupled Fe(III)/Fe(II) redox cycling and Fe(II) transport mediated by soil microbes. However, a full, comprehensive mechanistic picture of this phenomenon with necessary technical details still remains unavailable. We here provide a formulation of such a picture for Fe(III) film formation, as

schematically depicted in Figure 5 and presented with elaborations below, integrated with the results of our own experimental work.

Sequential Reactions (R) and Processes (P) of Microbially Mediated Generation of Floating Fe(III) Films

- R1: Aerobic Microbial Respiration**
 $C_6(H_2O)_6 + 6O_2 \rightarrow 6CO_2 + 6H_2O$
- P1: Complete Depletion of Dissolved Oxygen (DO) in Soil and Water**
- R2: Anaerobic Microbial Respiration and Reduction of Fe(III) (Insoluble) to Fe(II) (Soluble) at Soil/Water Interface**
 $C_6(H_2O)_6 + 24Fe(III) + 6OH^- \rightarrow 24Fe(II) + 6CO_2 + 18H^+$
- P2: Diffusion of Fe(II) to Water Surface**
- R3: Oxidation of Fe(II) to Fe(III) at Water/Air Interface**
 $4Fe(II) + O_2 + 2H^+ \rightarrow 4Fe(III) + 2OH^-$
- R4: Hydrolysis of Fe(III)**
 $Fe(III) + 3H_2O \rightarrow Fe(OH)_3 + 3H^+$
- R5: Polymerization of Fe(OH)₃ from Dimers to Polymers**
 $nFe(OH)_3 \rightarrow \{Fe(OH)_3\}_2 (n = 2) \rightarrow \{Fe(OH)_3\}_n$
- R6: Transformation of Fe(III) Film Polymers via H₂O Elimination**
 $\{Fe(OH)_3\}_n (\text{thin}) \rightarrow FeOOH (\text{thicker}) \rightarrow Fe_2O_3 (\text{crust})$

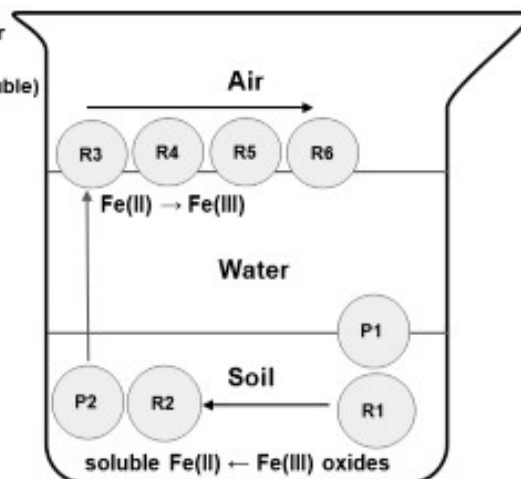
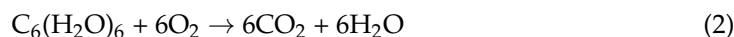


Figure 5. A schematic presentation of the hypothesized mechanistic picture proposed to depict the microbially mediated generation of floating Fe(III) films in a laboratory setting and on the water surface of natural aquatic systems. The entire film generation phenomenon contains a sequence of six biotic and abiotic (chemical) reactions (R1–R6) coupled with two physical processes (P1–P2).

The entire chain of events for floating Fe(III) film formation contains a sequence of six biotic and abiotic (chemical) reactions (R1–R6) coupled with two physical processes (P1–P2) in the soil–water system, as shown in Figure 5. This view is consistent with the general conceptual model constructed for the redox transformation of the Fe(III)/Fe(II) couple at oxic/anoxic boundaries [26,34,37].

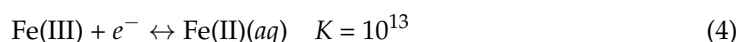
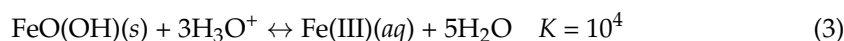
Chronologically, in a moist environment such as the inundated soils in our laboratory setting (Figures 2–4), the glucose added (sugar or monosaccharide as fast food or a quick energy source) jump-starts the flourishing of the aerobic soil microbes present in the fresh soil samples. Microbial activities and growth at high speed sustained by an unusually high supply of energy (sugar) eventually deplete the dissolved oxygen (DO) in the water within and above the soil (P1: complete depletion of DO in soil and water) [43] as a result of aerobic microbial respiration (R1) with the DO as the electron acceptor:

R1: Aerobic microbial respiration

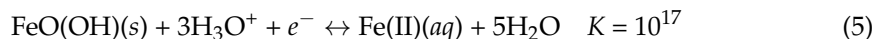


P1: DO depletion in soil and water

The aerobic condition: In the presence of dissolved oxygen, $O_2(aq)$ (i.e., the aerobic condition), the level of Fe(II) is negligible under the equilibrium condition involving the Fe(III)/Fe(II) redox couple. Considering a form of Fe(III) commonly present in natural aqueous environments, i.e., FeO(OH) (ferric oxyhydroxide), the level of Fe(II) is governed by the two equilibria shown below [17]:



The combination of R(3) and R(4) gives rise to the redox reaction for the Fe(III)/Fe(II) redox couple:



$$K = \frac{[\text{Fe(II)}](aq)}{[\text{H}_3\text{O}^+]^3 [e^-]} \quad (6)$$

where the symbol *aq* denotes the aquo complex of the metal cation in an aqueous medium and *s* stands for the solid phase (by convention, the solid state (i.e., FeOOH(*s*)) and pure water do not appear in an equilibrium equation (Equation (6)), since these concentration items, being constants based on their densities, are included in the *K* value for the equation). The above equation (Equation (6)) for the overall Fe(III)/Fe(II) redox couple (half redox reaction) can be transformed into log form:

$$\log[\text{Fe(II)}(aq)] = \log K - 3\text{pH} - pe \quad (7)$$

where $\text{pH} = -\log[\text{H}_3\text{O}^+]$, $pe = -\log[e^-]$, and e^- is for electron. At the *pe* level for air-saturated water (fully aerobic condition, $pe = 12.5$) and the circumneutral pH ($\sim\text{pH } 7$), we have $\log[\text{Fe(II)}(aq)] = -16.5$ ($\log[\text{Fe(II)}(aq)] = 17 - 3 \times 7 - 12.5$), i.e., $[\text{Fe(II)}(aq)] = 10^{-16.5} \text{ M}$ [17]. It is clear that under aerobic conditions, Fe(III) is predominant and the Fe speciation and the levels of Fe(III) and Fe(II) are controlled by the level of DO.

The anaerobic condition: Presumably, with aerobic decomposition of organic matter in operation, only $\sim 3.1 \text{ mg/L}$ of dissolved organic carbon (DOC) is needed to consume 8.25 mg/L of dissolved O_2 (note: under saturation of DO in water with atmospheric oxygen at a total atmospheric pressure of 1 atm and 25°C , saturated DO level in water = 8.25 mg/L or $2.58 \times 10^{-4} \text{ M mol O}_2/\text{L water}$, or $258 \mu\text{M}$, at the atmospheric O_2 level = $286 \text{ mg O}_2/\text{L air}$ for 21% of O_2 in the air). It was found that groundwater in a temperate climate region containing $> \sim 4 \text{ mg/L}$ of DOC (or total organic carbon (TOC), biochemical oxygen demand (BOD), chemical oxygen demand (COD)) will usually turn anaerobic. This finding (as a rule of thumb) generally applies to water in various places, such as stream-bottom muds, lake and reservoir bottoms, organic-rich waste ponds, water-logged soils, and deeper groundwater systems [43,44].

In our case, for example, $\sim 0.1 \text{ g}$ glucose was added to $\sim 40 \text{ mL}$ water, which amounts to a level of 1000 mg C/L in the system (i.e., 40 mg C in 40 mL water ; molecular mass for glucose: $\text{MM} = 180.156 \text{ g/mole}$; 6 C/glucose). This high level of glucose (or DOC) thus surely is destined to secure an anaerobic condition in the system at equilibrium.

According to Berner's practical redox classification based on water DO level [45], a DO level above $30 \mu\text{M}$ dictates an oxic environment with various Fe(III) species present predominantly and the DO level below $1 \mu\text{M}$ DO for an anoxic environment ($\text{DO} \geq 1 \mu\text{M}$: suboxic; $\text{DO} < 1 \mu\text{M}$: postoxic with Fe(II) present) [43].

At the beginning, the water above the soil sample contains some dissolved oxygen, which provides and sustains an aerobic condition under which the aerobic microbes are active. With glucose present, the aerobic microbial respiration becomes intensified to keep driving the consumption of DO. Eventually, the DO in the system is depleted, which then triggers the next steps in the chain of events:

R2: Anaerobic microbial respiration

Anaerobic reduction of Fe(III) oxides (in inundated soil or sediment)



P2: Fe(II) diffusion from soil to water surface

The depletion of DO shuts down the aerobic microbial activities and growth, which awakens the anaerobic microbes and their activities in the soil, as now, the conditions are anaerobically favorable [35,46]. Their respiration (R2) is running at full swing, and sooner

or later comes to the stage of enlisting of ferric iron, Fe(III), present in the Fe oxides and oxyhydroxides of the soil, as the electron acceptor along the redox ladder coupled with anaerobic respiration in soil and water [19,26,33,43,47,48].

Ferrous iron, Fe(II), is then generated during anaerobic microbial respiration at the soil/water interface. Soluble and thus mobile, the Fe(II) then diffuses and migrates to the water surface, the water/air interface (P2: migration of Fe(II) from soil to water surface) as the building-up of Fe(II) around the soil Fe(III) oxides and oxyhydroxides (as coating on soil clay particles, or as whole particles) is establishing an upward Fe(II) gradient.

The timespan for the chain of events of R1, P1, R2, and P2 kinetically amounts to the overall duration before the Fe(III) films start emerging at the water surface. This timespan sets the major kinetic limiting factor for floating Fe(III) film formation and can reach 1–2 days, depending on the specific microbial communities present and various conditions in the submerged soil system.

Hence, anaerobic microbial reduction of Fe(III) to Fe(II) is a key step in the overall process (chain of events) of Fe(III) film formation. Microbial enzymatic metal reduction, including reduction of Fe(III) in Fe(III) oxyhydroxides and oxides in soils and waters, is widely recognized [10,35,36,47–54] and may account for much of various metal reductions that occur in soils and sediments [35,51,52].

Reduction of the Fe(III) of soil iron oxides/oxyhydroxides to Fe(II) by soil anaerobic microbes: The dissimilatory Fe(III) reduction microorganisms commonly metabolize the organic carbons generated from fermentable sugars (e.g., glucose in our study), but they mainly use Fe(III) as the terminal electron acceptor in anaerobic respiration (dissimilatory microbial Fe(III) reduction), rather than as an energy source, or for the benefit of usage (uptake) of iron as a nutrient (assimilatory microbial Fe(III) reduction) since they usually can survive and grow in the absence of Fe(III) [51]. Soils with sufficient organic matter exhibit Fe(III) reduction more commonly, and low pH seems to favor the reduction [35,36].

Dissimilatory Fe(III) reduction is not particular to a single genus. Microbial Fe(III) reducers encompass a variety of microbes, including a large heterogeneous group of the heterotrophic bacteria. Among known Fe(III) reducers are *Alcaligenes*, *Bacillus*, *Clostridium*, *Desulfovibrio*, *Desulfuromonas acetoxidans*, *Geobacter metallireducens* (or GS-15), *Klebsiella*, *Proteus*, *Pseudomonas*, *Serratia*, and *Shewanella putrefaciens* [10,35,49], and other microbes of bacterial and fungal genera [47]. In a study in which the Fe(III) films were generated by progressive enrichment and incubation of the field sediment samples, the heterotrophic bacteria of the genus *Enterobacter* were found to be the dominant bacteria responsible for the generation of floating films, and the bacteria represented only a minor part of those microbial communities in the field [40]. A variety of sulfate-reducing microbes, such as *Desulfovibrio*, are capable of reducing Fe(III) as well [10].

Shewanella putrefaciens and *Geobacter metallireducens* (GS-15) are widely present in the environment, but *S. putrefaciens* is more commonly found in sedimentary environments, while GS-15 is mostly predominant in soils [10,55]. Both *S. putrefaciens* and GS-15, like sulfur-reducing bacteria, utilize the metabolic products of other microorganisms, e.g., amino acids, formate, acetate, butyrate, propionate, and some long-chain fatty acids, to oxidize food to CO₂ to harvest energy, meanwhile using Fe(III) as the electron acceptor by reducing Fe(III) to Fe(II) [10,46]. Some microbes (e.g., *Micrococcus lactilyticus*) can even use molecular hydrogen (H₂) to reduce ferric hydroxide and ferricyanide [36,56].

Metabolic studies of glucose in sediments with Fe(III) as the electron acceptor for respiration showed that glucose was fermented first to organic acids (primarily acetate), then followed by oxidation of these acids to CO₂. Fermentative microbes first metabolize available sugars (and amino acids) to short-chain fatty acids and H₂ and the products of the fermentation are then consumed by the Fe(III)-reducing microbes accompanied by Fe(III) reduction via anaerobic respiration [46,51]. Generally, anaerobic activities (called anaerobiosis) of fermentative microbes can result in accumulation of organic acids, with acetic, formic, and butyric acids as the dominant acids (lactic and succinic acids as the minor ones) [35,48].

Our study showed that shortly after the tested system with added glucose was set to run, many bubbles, together with a fermentation odor, occurred, as described before. These observations echo the microbial and metabolic processes described above. The gases in the bubbles are considered to be CO₂ from the fermentation. Hence, fermentation serves as a signal for the subsequent formation of Fe(II) via microbial Fe(III) reduction.

Anaerobic reduction of Fe(III) by metal-reducing bacteria using endogenous Fe(III) oxides as the primary electron acceptor source occurs widely in the environment ([51,57,58]. Bacteria (e.g., *Bacillus*) and fungi (e.g., *Alternaria* and *Fusarium*) were found to be able to reduce Fe(III) enzymatically [58] (for more examples, see [51]). In a kinetic study in which Fe(III) reduction was followed using synthetic crystalline Fe(III) oxide (goethite) and two southern Fe(III) oxide-rich subsoils from Tennessee and North Carolina (USA) in the cultures of the Fe(III)-reducing bacterium *Shewanella alga* strain BrY, significant Fe(III) reduction to Fe(II) was found, and removal of Fe(II) through aqueous phase transport was shown to prominently control the rate and extent of Fe(III) reduction [57]. As a result of the assistance of the advective removal of Fe(II), crystalline Fe(III) oxides were found to be consumed nearly completely within a shallow subsurface landfill leachate plume in Denmark [57,59]. In our study, the upward migration of the generated Fe(II) towards the water surface should also serve as an effective aqueous transport venue to enhance the biotic reduction of solid-phase Fe(III) species.

It is clear that a group of players are at the center of this activity, including (1) water (as O₂ barrier), (2) Fe(III) oxides/oxyhydroxides (Fe(III) source), (3) Fe(III) reducers and other microbes to generate acetate as food for the Fe(III) reducers, and (4) sugar (food for fermentation microbes). They work collectively in a chain of biotic and chemical events to stage the biotic Fe(III) reduction. The role of sugar is critical. It is the acetate generated by fermentative microbes using sugar, which triggers the activity and flourishing of the Fe(III) reducers. Our study showed that in the absence of sugar, absence of Fe(III) film or little film was observed, and no bubbles or odor occurred.

Electron transfer during anaerobic microbial reduction of Fe(III) to Fe(II): Electron transfer occurs during anaerobic respiration, involving microbial reduction of Fe(III) to Fe(II), as depicted by a biotic mechanistic model for the processes and pathways operative in Fe(III) reduction [51,52]. Three mechanisms were revealed to account for the electron transfer between microbial cells and Fe(III)-containing solid particles: (1) direct physical contact between the cells and the Fe(III) particles (or particle surfaces, or both) in addition to cellular Fe(III) reductase(s), (2) extracellular (external) electron shuttles either generated microbially or available environmentally to transfer the electron(s) from electron donor (organics in cells) to Fe(III) in the solid particles, and (3) dissolution of Fe(III) solids by complexing Fe(III) with microbially generated ligands. Different species of microbial Fe(III) reducers may use different mechanisms [48,51,52,60].

Regarding direct physical contact between microbial cells and Fe(III) particles, the actual transfer of electrons from cells involves an electron transfer chain that may enlist one (or more) electron carrier(s) (e.g., some metal ion(s)) [51]. Actually, the microbes can also be adsorbed on the Fe(III) particle surfaces, in addition to the case where the microbes are simply physically mixed with Fe(III) particles. The adsorption of the microbes can provide close, or closer, contact between the microbial cells and Fe(III) solid particles and thus enhance the electron transfer.

Insoluble Fe(III) species can pose a challenge to Fe(III) reducers during the transfer of reducing equivalents from microbial cells to Fe(III) solids in anaerobic respiration by means of Fe(III) solids serving as the ultimate electron acceptors [50,60]. The *Shewanella* species was found to evolve to tackle this challenge by enlisting quinones or flavins as electron shuttles between cells and substrates. However, some distance is still inevitable between the cells and Fe(III) particles. For the *Geobacter* species, direct physical contact that allows for the passing of electrons from a bacterial biofilm directly to the Fe(III) is necessary between the cells and substratum. This biofilm–mineral contact could also be facilitated

by pili or microbial nanowires, which can provide metallic-like conductivity and mediate electron transfer [48,50,52,61].

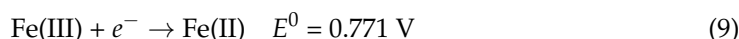
Two types of electron shuttles have been recognized as being capable of facilitating microbial Fe(III) reduction: (1) exogenous electron shuttles and (2) endogenous electron shuttles. Exogenous shuttles are already present in the environment outside cells. One of these extracellular shuttles are humic substances with a variety of aromatic structures and other quinone-like organic compounds in the reduced form of hydro-quinones. It is known that the endogenous shuttles are produced by microbes and then released to the surrounding environment to serve as electron transfer facilitators. For example, *Geothrix fermentans* can supply a quinone-like electron shuttle for their growth on lactate (electron donor or food for the microbes) mixed with Fe(III) particles (electron acceptor) [53,62].

Additional features of microbial reduction of Fe(III) species to Fe(II): The degree of crystalline structure formation plays a special role in microbial Fe(III) reduction. The Fe(III)-reducing microbes appear to favor less crystalline Fe(III) oxides, and it seems that less crystalline structures are more amendable or vulnerable to enzymatic attack during microbial Fe(III) reduction [51]. Some Fe(III) species can be reduced enzymatically in cell-free systems or even reduced by metabolic end-products abiotically [47]. In addition to enzymatic reduction of Fe(III) in soils and sediments, non-enzymatic Fe(III) reduction may also contribute to the overall anaerobic microbial Fe(III) reduction. Yet, the enzymatic reduction is more predominant than the non-enzymatic reduction and it can oxidize the organic compounds completely to CO₂ [51].

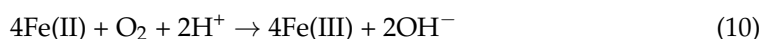
It needs to be pointed out that the chemical reaction equation for the Fe(III)/glucose couple (R(8)) does not suggest a reaction actually occurring between Fe(III) and glucose. It instead offers a stoichiometric estimation of the electrons transferred from glucose to Fe(III) during anaerobic respiration by assuming all glucose added and all electrons from the oxidation of the added glucose are consumed solely by Fe(III) in the oxidation. In our study, some of the added glucose was first consumed by aerobic microbes to deplete DO to create an anaerobic condition for the subsequent fermentation to occur.

After being microbially generated, at the end of the upward transport, Fe(II) finds itself at the water/air interface (a redox interface, or redox front, across which a rather abrupt or steep change in redox potential Eh occurs [43]), now in a favorable niche for its oxidation back to Fe(III), i.e., a wealth of DO and a circumneutral pH condition (~pH 7, mediated by CaCO₃ added). There, Fe(II) is readily oxidized back to Fe(III) rather quickly (R3) [63]:

R3: Fe(II) oxidation



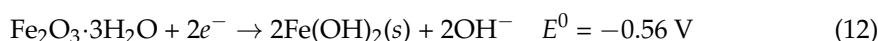
Under acidic conditions:



or



Under basic conditions, for example, the oxidation is still readily favorable:



The hexaquo ferrous ion Fe(II)(H₂O)₆²⁺ bears a high spin and a transition around 1000 nm, with an absorption band tail extended to the visible region towards the red end, which is responsible for the pale blue-green color of the Fe(II) solution. Aqueous Fe(II) hydrolyzes only slightly [64].

Kinetics of Fe(II) oxidation: The rate of Fe(II) oxidation depends on the level of DO (i.e., O₂(aq.)) and pH, as well as the concentration of Fe(II) in the system. The oxidation of Fe(II) was shown to exhibit the first-order kinetics with respect to both the Fe(II) and O₂

concentrations, and second-order with respect to $[\text{OH}^-]$. This points to a 100-fold rise in the Fe(II) oxidation rate upon a rise in pH by one unit. The detailed kinetics of Fe(II) oxidation has been revealed [26]. The oxidation is strongly pH-dependent kinetically; it is slow at $\text{pH} < 6$. The oxidation of Fe(II) was found to follow the kinetics shown below [65–67]:

$$-d[\text{Fe(II)}]/dt = k[\text{Fe(II)}][\text{OH}^-]^2 p_{\text{O}_2} \quad (13)$$

where $k = 8.2 \pm 2.5 \times 10^{13} \text{ min}^{-1} \text{ atm}^{-1} \text{ mol}^{-2} \text{ L}^2$ at 20°C . An alternative form of the kinetic rate equation can be obtained below:

$$-d[\text{Fe(II)}]/dt = k_{\text{H}}([\text{O}_2(\text{aq})]/[\text{H}^+]^2)[\text{Fe(II)}] \quad (14)$$

where $k_{\text{H}} = 3 \times 10^{-12} \text{ min}^{-1} \text{ mol L}^{-1}$ at 20°C .

An elaboration of the Fe(II) oxidation and its kinetic picture is given as follows: in the presence of DO and at circumneutral pH, oxidation can proceed at a fairly fast rate. For a general redox half reaction, $\text{red}_1 + \text{ox}_2 \rightarrow \text{red}_2 + \text{ox}_1$, its rate law equation takes the general form of $\text{rate} = k[\text{red}_1][\text{ox}_2]$. For a simplified general conceptual redox half reaction for Fe(II) oxidation, $\text{Fe(II)} + \text{O}_2 \rightarrow \text{Fe(III)}$, likewise, the oxidation thus can be expressed as $\text{rate} = k[\text{Fe(II)}][\text{O}_2]$. Hence,

$$\text{rate} = -d[\text{Fe(II)}]/dt = k'[\text{Fe(II)}][\text{O}_2] \quad (15)$$

At a fixed level of oxygen, which can occur in natural environments, $[\text{O}_2]$ can be treated as a constant; thus, combining k' and $[\text{O}_2]$ yields pseudo first-order kinetics:

$$\text{rate} = k_{\text{obs}}[\text{Fe(II)}] \quad (16)$$

where $k_{\text{obs}} = k'[\text{O}_2]$. Wehrli et al. [68] showed that the Fe(II) oxidation kinetics also depends on solution pH, as they found a logarithmic relationship between k_{obs} and $[\text{H}^+]$ (i.e., $\log k_{\text{obs}}$ vs. pH being linear). This pH dependence is a manifestation of the effect of pH-dependent aqueous Fe(II) speciation, since Fe(II) exists in several hydrolyzed forms in water (total $[\text{Fe(II)}] = [\text{Fe}^{2+}] + [\text{FeOH}^+] + [\text{Fe(OH)}_2]$):

$$\text{rate} = k_{\text{obs}}[\text{Fe(II)}] = k_0[\text{Fe}^{2+}] + k_1[\text{FeOH}^+] + k_2[\text{Fe(OH)}_2] \quad (17)$$

A kinetic equation for Fe(II) oxidation with oxygen incorporated (in addition to the effect of pH) can thus be given:

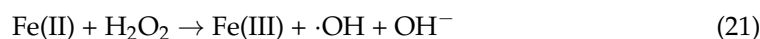
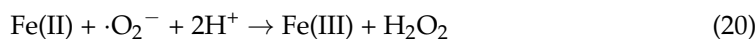
$$\begin{aligned} \text{rate} &= -d[\text{Fe(II)}]/dt = k'[\text{Fe(II)}][\text{O}_2] = k_{\text{obs}}[\text{Fe(II)}] \\ &= k_0'[\text{Fe}^{2+}][\text{O}_2] + k_1'[\text{FeOH}^+][\text{O}_2] + k_2'[\text{Fe(OH)}_2][\text{O}_2] \end{aligned} \quad (18)$$

where $k_{\text{obs}} = k'[\text{O}_2]$, $k_0 = k_0'[\text{O}_2]$, $k_1 = k_1'[\text{O}_2]$, and $k_2 = k_2'[\text{Fe(OH)}_2][\text{O}_2]$ [33].

The pH dependence of Fe(II) oxidation can be explained by the following theory: first, hydrolyzed Fe(II) species are more favored, with faster Fe(II) oxidation rates than nonhydrolyzed ones; second, the OH^- ligands associated with Fe(II) in the hydrolyzed Fe(II) species can donate electron density to Fe(II), which makes Fe(II) more reducing.

Mechanism of Fe(II) oxidation: Mechanistically, oxidation of Fe(II) to Fe(III) involves an outer-sphere electron transfer through both σ and π systems of O_2 and Fe(II) species. The OH^- ligands associated with the hydrolyzed Fe(II) can stabilize the oxidized Fe, i.e., the Fe(III) species [26,28,69], as detailed in a mechanistic scheme for Fe(II) oxidation by Schneider and Schwyn [11]. Fe(II) oxidation involves several active oxygenated species, including the following: superoxide ($\cdot\text{O}_2^-$), hydroxide free radical ($\cdot\text{OH}$), and hydrogen peroxide (H_2O_2), catalytically as well as non-catalytically. H_2O_2 is relatively stable and thus a detectable product during Fe(II) oxidation [70,71].

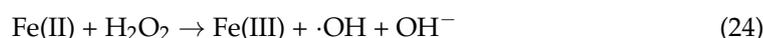
The Haber–Weiss mechanism has been adopted to formulate the mechanism for aqueous Fe(II) oxidation by oxygen, which is the most accepted mechanistic model for Fe(II) oxidation [67,72]:



The Fenton reaction is shown below (i.e., R(23) and R(24); the Fenton reagent Fe(II) + H₂O₂) [73] also plays a notable role in Fe(II) oxidation [26]:



or



Both H₂O₂ and ·O₂[−] can be considerably active during Fe(II) oxidation, since they can be generated at significant levels, especially at oxic–anoxic interfaces (air/water interfaces) where O₂ is readily available [70].

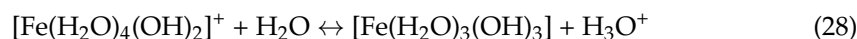
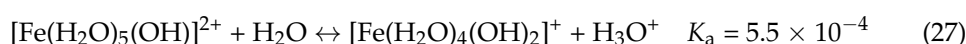
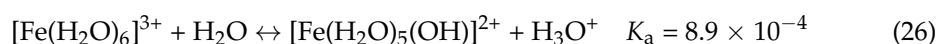
Immediately after the oxidation of Fe(II) to Fe(III), under the favorable condition of circumneutral pH, Fe(III) can readily hydrolyze to form Fe(III) hydroxides (R4):

R4: Fe(III) hydrolysis



Hydration of Fe³⁺ cation: In an aqueous solution, like any cation to be stabilized in the highly polar medium of water, cation Fe³⁺ (generally represented by Fe(III) without its actual form(s) present in water being specified) actually stays as a hydrated cation, also called aquated cation [74], bound to six water molecules (i.e., [Fe(H₂O)₆]³⁺) [17,75]. Hence, [Fe(H₂O)₆]³⁺ is an octahedral coordination compound with water as the ligand bound to the central metal cation Fe³⁺ (Figure 6).

Hydrolysis of Fe(III) species: Aqueous multivalent metal ions are known to undergo a sequence of consecutive proton (H⁺) transfers and thus become Brønsted acids [26]. The aquo Fe(III) compound (hydrated Fe(III)) bears a shift in electron density to Fe³⁺ from the OH bonds of the coordinated water ligands. This shift leads the protons of the OH groups of the water molecules to become acidic and consequently results in their dissociation (i.e., hydrolysis) [17,75] (see Figure 6 for R(26)):



The above sequence depicts the hydrolysis reactions of Fe³⁺(aq) cation in aqueous media (aquo Fe(III)) readily occurring at pH > ~1 [8,63,64,75,76]). A charge increase and a size decrease in cations can enhance their polarizing power and tendency to hydrolyze [77].

At a higher solution pH, the Fe(III) species then hydrolyze (also called protolyze) further from R(26) up to R(28), faster and to a larger extent. Only at pH = ~0 (or pH < 1), ~99% of Fe(III)(aq) may be expected to stay as [Fe(H₂O)₆]³⁺, a pale purple hexaquo cation [63,74]. The Fe(III) hydrolysis products can exist first in various mononuclear complexes with a general formula of Fe(OH)_x(H₂O)_yⁿ⁺ (x = 1, 2, 3, and 4; n = −1, 0, 1, 2), for example, Fe(OH)(H₂O)₅²⁺, Fe(OH)₂(H₂O)₄⁺, Fe(OH)₃(H₂O)_y, and Fe(OH)₄(H₂O)_x[−] [11]. The first Fe(III) hydrolysis product from the purple hexaquo [Fe(H₂O)₆]³⁺ cation (a complex) is the yellow [Fe(H₂O)₅(OH)]²⁺. This features charge-transfer UV absorption bands with an extended absorption tail in the visible region that gives it its yellow color [64].

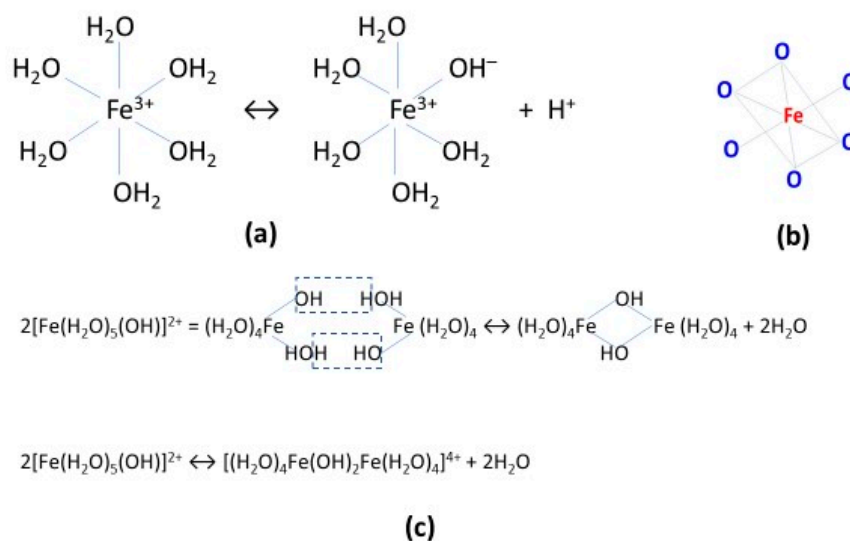


Figure 6. A schematic presentation (a) of the hydrolysis of Fe(III) cation (Note: The Fe(III) cation here is a general term adopted to refer to various representations for Fe(III) cation in an aqueous solution, e.g., hydrated Fe(III) cation, aquated Fe(III), $\text{Fe}^{3+}(\text{aq})$, aquo Fe(III), or hexaquo Fe(III), with all the various denotations representing $[\text{Fe}(\text{H}_2\text{O})_6]^{3+}$ as an octahedral coordination compound with H_2O molecules as the ligands bound to the central metal cation Fe^{3+} as shown by (b), specifically for the bonding between O and Fe in the octahedral geometry of the $\text{Fe}(\text{III})\text{O}_6$ unit in various Fe(III) polymers subsequently formed following Fe(III) hydrolysis. Only the first step of the hydrolysis of Fe(III) is shown here) and (c) of the polymerization of the Fe(III) hydrolysis products ($[\text{Fe}(\text{H}_2\text{O})_5(\text{OH})]^{2+}$) to form an Fe(III) dimer ($[(\text{H}_2\text{O})_4\text{Fe}(\text{OH})_2\text{Fe}(\text{H}_2\text{O})_4]^{4+}$) by the condensation polymerization via elimination of water molecules.

The chemical formula (composition/stoichiometry) and actual structures of the Fe(III) species in liquid water solution also depend on the ionic strength and companion anions (or ligands and complexes of Fe(III) formed with the ligands) of the tested Fe(III) solution as well as the concentration of the Fe(III) in the solution [74,78,79]. The reactions of the hydrolysis and eventual precipitation of aqueous Fe(III) include formation, aging, and then agglomeration of a red cationic hydrolytic polymer [76].

The chemical term ferric hydroxide(s) ($\text{Fe}(\text{OH})_3$) by no means depicts chemically well-defined Fe(III) compounds. Instead, it represents a virtually unrestricted variety of Fe(III) species that differ in broad aspects, such as composition, structure, particle shape, size, distribution, interfacial characteristics, and thus chemical reactivity [11].

Various stages of Fe(III) hydrolysis: Hydrolysis of aqueous inorganic Fe(III) spans three sequential stages: (1) formation of low molecular mass hydrolysis species (e.g., $\text{Fe}(\text{OH})^{2+}$, $\text{Fe}(\text{OH})_2^+$, $\text{Fe}(\text{OH})_3$, $\text{Fe}_2(\text{OH})_2^{4+}$ dimer), (2) formation of a red cationic polymer (general structural scheme: coordination number six for Fe(III) in an octahedral complex of $\text{Fe}(\text{O}, \text{OH}, \text{H}_2\text{O})_6$ or $\text{Fe}(\text{III})\text{L}_6$, $\text{L} = \text{O}, \text{OH}$, or/and H_2O ; $\text{Fe}(\text{III})\text{--O}$ distance for crystals: 0.2 nm), and (3) aging of the Fe(III) polymers, followed by ultimate transformation to various Fe(III) oxides, and in various cases, to precipitation of the Fe(III) oxide phases directly from the low molecular mass precursors. It needs to be noted that most studies on Fe(III) hydrolysis have been conducted by adding bases to Fe(III) salts (e.g., nitrate, perchlorate, chloride, sulfate, etc.) [76].

Various kinds of Fe(III) hydrolysis: The companion anions (ligands) from the Fe(III) salts used in the Fe(III) hydrolysis studies that are inevitably present in the hydrolysis solutions are influential to the Fe(III) hydrolysis processes, formation of various particular hydrolysis products, and then subsequent polymerization of these products [76].

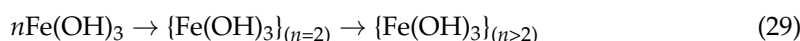
There are two kinds of Fe(III) hydrolysis: (1) hydrolysis occurring in inorganic Fe(III) salts exposed to a (strong) base (e.g., NaOH) added at (quite) high concentrations and (2) hydrolysis occurring in Fe(III) generated at around circumneutral pH from oxidation

of Fe(II) microbially produced anaerobically. Hence, the Fe(III) hydrolysis processes and products, following polymerization of Fe(III) hydrolysis products, and the subsequent formation, growth, and aging of floating Fe(III) films may not resemble each other for these two kinds of Fe(III) hydrolysis. Fe(III) hydrolysis originating from oxidation of Fe(II) may differ kinetically and mechanistically from that via a direct interaction of an Fe(III) salt with a (strong) base in the presence of inorganic anions (e.g., chloride, perchlorate, bicarbonate, sulfate, nitrate), or organic ligands (e.g., acetate, lactate, oxalate), especially at high concentrations of Fe(III) salts and/or the companion anions or ligands [11,79].

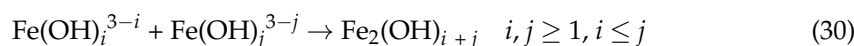
In our study, two special conditions are notable: (1) the setting is natural, with fresh soil in water; (2) Fe(III) is generated via natural microbial Fe(III) reduction and subsequent re-oxidation of the Fe(II) thus slowly generated and supplied in the setting with natural companion components at natural levels (both Fe(II) and Fe(III) occurring at slow rates). The natural setting and conditions may collectively contribute to the occurrence of floating Fe(III) films, as observed in nature and in our laboratory.

In an aqueous solution at around circumneutral pH, individual Fe(OH)₃ monomers become unstable and proceed to polymerize (R5):

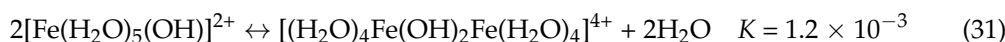
R5: Polymerization of Fe(OH)₃ and various other Fe(III) hydrolysis products



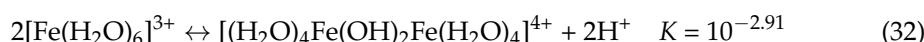
General process of polymerization of Fe(III) hydrolysis products: Upon hydrolysis of Fe(III), polymerization of single, discrete molecules of its hydrolysis products occurs (R(26)–R(28)) with various Fe(III) polymers formed depending on pH [75]. One general, schematic representation of Fe(III) polymerization can be given [11]:



The polymeric hydrolysis products (iso-polycations) can be multinuclear, and their existence is common for most metal ions [26]. For example, a dimer can be formed for the first Fe(III) hydrolysis product (see R(26)) as shown below and in Figure 6 [16,17,79]:



Fe(III) dimer forms by condensation between the two monomers via elimination of H₂O. This is why two H₂O molecules are generated as products appearing on the right side of equation R(31). Another way to show Fe(III) dimer formation is as follows [63]:



The Fe(III) dimer Fe₂(OH)₂⁴⁺, or [(\text{H}_2\text{O})₄Fe(OH)₂Fe(\text{H}_2\text{O})₄]⁴⁺, is essentially diamagnetic [79,80]. In the symmetrical assembly of the Fe(III) dimer, the two Fe(III) cations are joined by a double bridge of Fe–O–Fe with each Fe bound to two oxygens of the two central OH groups (Figure 6, O shared between two Fe(III) ions). These polymer structures are called bridged polynuclear (multinuclear) polymer species. The existence of the Fe(III) dimer has been verified [26]. The hydroxoiron(III) dimer (Di-μ-hydroxo-octaaquodiiron(III), Fe₂(OH)₂⁴⁺) has been characterized [81]. The dimerization of Fe(III) hydrolysis products was found to proceed kinetically as shown below, e.g., for a simple dimerization reaction:



with the dimerization rate constant reported at 450 (±50) M⁻¹ s⁻¹ and the decomposition (backward reaction) rate constant at 1 (±0.5) s⁻¹ (25 °C, ionic strength I = 0.6) [81].

Mechanism of polymerization of Fe(III) hydrolysis products: Hydroxo-aquacations polymerize to generate polynuclear hydroxo-bridged cations [82]. The polymerization of various Fe(III) hydrolysis products can proceed further to generate highly polymerized Fe(III) species with various intermediate products, depending on pH and time and thus

more bridges of Fe–O–Fe can form through the OH groups by means of condensation via elimination of H₂O. The terms “ol” and “oxo” are generally adopted to refer to the –OH– and –O– bridges. The formation processes of these bridges are called olation and oxalation. Olation then may be followed by oxolation in which the bridging OH group is turned into a bridging O group [26].

Ultimately, some water molecules and protons are split during Fe(III) hydrolysis [17]. The elimination of water molecules to form polymeric bridges (or links) during the polymerization is the condensation process [76]. Condensation (polymerization) occurs during the sequence of Fe(III) hydrolysis and the polymerization of various hydrolysis products from aquo- to hydroxo- to hydroxo-oxo to oxo complexes of Fe(III) [26].

This condensation via H₂O elimination (Figure 6) is mechanistically fundamental and highly important in the polymerization of various Fe(III) hydrolysis products. Essentially, Fe(III) hydrolysis products can form various Fe(III) polymers from linear polymers (e.g., a dimer or a trimer, etc.) to 2D polymer sheets and finally to 3D Fe₂O₃ solids via this single fundamental mechanism alone.

Further stages of polymerization of Fe(III) hydrolysis products: With increase in pH above 2–3, more highly condensed Fe(III) polymer species beyond the Fe(III) dimer are generated, making an equilibrium harder to establish or even unattainable. Formation of colloidal gels of the various Fe(III) polymers with various structures soon follows [63]. For example, a polynuclear hydroxo complex was suggested to have 1–50 iron atoms in its polymer assembly, and ultracentrifuge measurements showed that these Fe(III) polymers could even reach a polymeric assembly of about 900 iron atoms [80].

Eventually, with increasing of pH, hydrous ferric oxides become precipitated to form a red-brown gelatinous mass in an aqueous solution when well mixed, or upon a rapid addition of large doses of base. It remains unclear whether ferric hydroxides may exist in a definite chemical form of Fe(OH)₃. The red-brown precipitates, commonly denoted as ferric hydroxides, are represented best by hydrous ferric oxide (Fe₂O₃·nH₂O) [63].

The composition and structure of the Fe(III) polymerization products depend on pH, total Fe content, and time. Fe(III) hydroxides in the apparent form of Fe(OH)₃, the neutral, polymerized, insoluble species, form more as orange amorphous precipitates. Fe(OH)₃ as a formula may not represent the real chemical form and structure of the precipitates. Fresh Fe(III) hydroxide polymers usually feature some uncertain structures (at various degrees of polymer condensation). With aging, the polymers mainly become FeO(OH). It is known that the structurally uncertain (indistinct) nature of fresh Fe(III) hydrolysis products (or polymers) usually results in highly gelatinous and often colloidal precipitates [17].

The nature of Fe(III) hydrolysis renders Fe(III) salts eventually insoluble in water at circumneutral pH (note: Fe(III) largely present as hydroxo complexes at pH ~4). Yet, Fe(II) species do not hydrolyze significantly until ~pH 10, soluble even around circumneutral pH, while at ~pH 8, the soluble Fe(III) level is already as low as 3×10^{-11} M [17]. Yet, in natural waters, the authentic Fe(III) level is considered to be $\sim 10^{-6}$ – 10^{-8} M, significantly higher than calculated from the Fe(III) solubility equilibria. These higher levels cannot be readily accounted for with expected certainty but are attributed to the involvement of the soluble complexes (coordination compounds) of Fe(III) of some unknown nature, likely associated with various natural organic ligands (e.g., fulvic acids, humic acids) in natural waters [17].

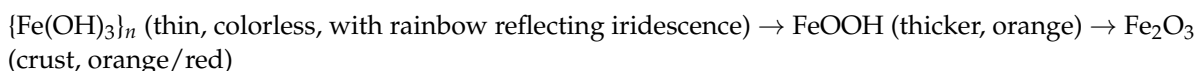
Kinetics of polymerization of Fe(III) hydrolysis products: Although the sequential hydrolysis of Fe(III) can readily reach the equilibria (or semi-equilibria, quasi-equilibria) rather quickly, various products of Fe(III) hydrolysis subsequently polymerize rather slowly. Kinetically, the polynuclear hydroxo Fe(III) complexes stay as thermodynamically unstable intermediates in a slow transition (up to weeks) from free aquo metal ions to colloids and eventually to solid precipitates with gradual structural transformations [26]. Some isolated Fe(III) polymers do not precipitate for an indefinite period, in spite of the well-known instability of hydrolyzed Fe(III) solutions. This seems to suggest that high activation energy is probably required for the formation of the various Fe(III) polymers as Fe(III) hydrolysis products transform to insoluble Fe(III) hydroxides [80].

Fe(III) polymers formed from various Fe(III) hydrolysis products are considered to be the initial forms of Fe(III) films. These subsequently undergo mineralogical changes to become Fe(III) oxyhydroxides (FeOOH) (R6) (also see R(34) shown below), followed by further transformation to Fe(III) oxides in the chemical and mineralogical journey of Fe(III) film formation and transformation:

R6: Transformation of Fe(III) film polymers via H₂O elimination:



With their change in thickness, the Fe(III) films also change their color, as shown by the following simplified sketch of the transformation and aging of Fe(III) films:



An elaborated formulation of the chemical and mineralogical transformation of Fe(III) films will be presented in a subsequent section.

3.4. Special Characteristics of the Floating Fe(III) Film Phenomenon

The mechanistic picture of the floating Fe(III) film formation formulated above shows that the Fe(III) film phenomenon is no random coincidence. Microbial mediation plays a pivotal role, and the required favorable conditions are also critical. The occurrence of Fe(III) films requires a slow, gradual pace that is maintained for each process in the chain of events during their formation: Fe(II) supply from microbial Fe(III) reduction, oxidation of Fe(II) to Fe(III), its hydrolysis to form Fe(III) monomers, and further polymerization, all on an appropriate scale (quantity) so as to prevent or derail flocculation and precipitation of Fe(OH)₃. A large amount of Fe(OH)₃ rushing into a solution (e.g., titrating Fe(III) with NaOH) can inevitably result in rapid flocculation and precipitation of Fe(OH)₃. Only the supply of a small, limited amount of Fe(III) monomers can secure a favorable circumstance for slow polymerization and then gradual formation of thin films on water surfaces.

Once formed, the floating film then prevents O₂ from entering the water, leaving the Fe(II) below the film with less DO for its oxidation to Fe(III), thus still remaining as Fe(II), which was observed and verified in our mechanistic study (reported in detail later). The floating film formation thus can slow down the generation of more Fe(III) hydrolysis products and Fe(III) polymers, which can amount to flocculation and precipitation of the Fe(III) species. This feedback acts as another control over the film formation pace.

The role of the microbial control in the Fe(III) film formation is twofold: first, the slow, gradual supply of Fe(II) is fulfilled by microbial reduction of Fe(III) species via anaerobic respiration. It appears that the microbes are capable of delivering an optimum supply of Fe(II) quantitatively as well as kinetically. Second, both anaerobic and aerobic microbes team up to maintain anaerobic status in the system as long as sufficient sugar is available. If the DO level surpasses the threshold, the aerobic microbes wake up to deplete the DO and restore the anaerobic condition, as if there were a DO control homeostasis or redox seesaw attended to collectively by the microbial communities. Hence, the microbial role in floating Fe(III) film formation can never be overappreciated.

In summary, the mystery of the floating Fe(III) film phenomenon is revealed to be an environmental chemical drama of Fe(III)/Fe(II) redox cycling coupled with Fe(II) transport and Fe(III)/Fe(II) transformation at soil/water and water/air interfaces in the system.

3.5. Experimental Tests to Probe the Process and Mechanism of the Floating Fe(III) Film Phenomenon

We conducted a set of tests to gain experimental evidence to support the mechanistic picture of the floating Fe(III) film phenomenon. Several controlling factors for the floating Fe(III) film phenomenon were identified: (a) glucose (sugar, energy source), (b) CaCO₃ (base, pH control), (c) water (depth, DO, redox control), and (d) oxygen (respiration, redox

control). Each factor was examined by using the same representative R4 soil (Table 3). Another set of work was performed to verify the existence of Fe(II) in the system and monitor its level over a wide timespan (April–May 2023). Efforts were made to use ferrous salt placed in an aqueous solution to generate floating Fe(III) films abiotically.

Glucose test: This test showed that in the absence of glucose, Fe(III) films did not occur (Table 9). This suggests that glucose was required and further indicates that certain microbial activities were involved in film formation. As discussed before, glucose plays a crucial role in firing up microbial activities and flourishing, and in turn, the initial aerobic and following anaerobic microbial respiration responsible for the depletion of dissolved oxygen and generation of Fe(II) in the soil/water system. Our latest study showed that a certain threshold level of glucose was operative for the occurrence of floating Fe(III) films.

Table 9. Results of the study on the microbial mediation involved in floating Fe(III) film generation (Expt.–3) in a setup with the representative R4 soil.

Glucose and CaCO ₃	Role of Microbial Mediation		
	Day 3	Day 5	Day 7
No glucose	No activity	No activity	No activity
Normal glucose	Thin film, iridescent	Thick crust, red colored	Thick crust, red colored
No CaCO ₃	No activity	No activity	No activity
Normal CaCO ₃	Thin film, iridescent	Thick film, red colored	Thick crust, red colored

CaCO₃ test: This test showed that with CaCO₃ absent, the films did not seem to occur (Table 9). This suggests that a mild (circumneutral) pH condition is favorable for the film formation and furthermore a pH condition favorable for the microbial activities (i.e., Fe(II) reduction), Fe(II) oxidation, and Fe(III) hydrolysis was required for the film generation. The role of CaCO₃ is expected to be more influential for acidic soils since these are more sensitive or vulnerable to pH change. One avenue for pH change is Fe(III) hydrolysis (R(26)–(28)). Interestingly, Fe(III) hydrolysis also functions as a negative feedback: it yields H⁺ (lowering pH), which, in turn, can retard further Fe(III) hydrolysis. CaCO₃ can interrupt or terminate this feedback loop by removing the H⁺ generated during Fe(III) hydrolysis.

Water level test: This test showed that films occurred for the various water levels used. However, it seems that higher water levels led to somewhat less films generated and slower change from thin films to thicker films and crusts (Table 10). This may be due to the dilution effect and/or longer diffusion path to the water surface, both of which can contribute to retardation of Fe(III) film formation and change.

Table 10. Results of the study on the effect of water level and O₂ on floating Fe(III) film generation (Expt.–3) in a setup with the representative R4 soil.

Water Level and O ₂	Role of Water and Oxygen		
	Day 3	Day 5	Day 7
High water	Thin film, red colored	Thin crust, red colored	Thick crust, red colored
Normal water	Thin film, red colored	Thick crust, red colored	Thickest crust, red colored
Low water	Thin film, iridescent	Dried up	Dried up
Headspace without O ₂ , beaker covered	No activity	No activity	No activity
Normal O ₂ supply, beaker not covered	Thin film, iridescent	Thick crust, red colored	Thick crust, red colored

Oxygen test: The particular test showed that with O₂ absent in the headspace above the water, the film did not occur. This suggests that an oxidation was indeed involved in association with O₂ required as a source of oxidizing agent (Table 10). As is known, Fe(II) oxidation to Fe(III) needs oxygen. A lack of oxygen in the headspace above together with depletion of DO in the water makes Fe(II) oxidation unamenable or impossible.

Film color change: The color change in the Fe(III) films from colorless to orange to orange-red/red (Figures 3 and 4, Tables 7 and 8) suggests that the films involve hydroxide, oxyhydroxide, and oxide of Fe(III), since these colors are typical of the Fe(III) compounds.

Occurrence and monitoring of Fe(II) during Fe(III) film formation: To further probe the mechanistic picture of the Fe(III) film formation, we measured the level of the Fe(II) generated during the formation process. This was performed by using the same setup used in the Second Test of Case Study (April–May 2023) (shown in Table 8 and Figure 4). The Fe(II) level in the standing solution beneath the Fe(III) film layer and above the submerged soil was monitored over a wide span of time (~46 days) to track the generation and status of the Fe(II) in the process of film formation and transformation (Figure 7).

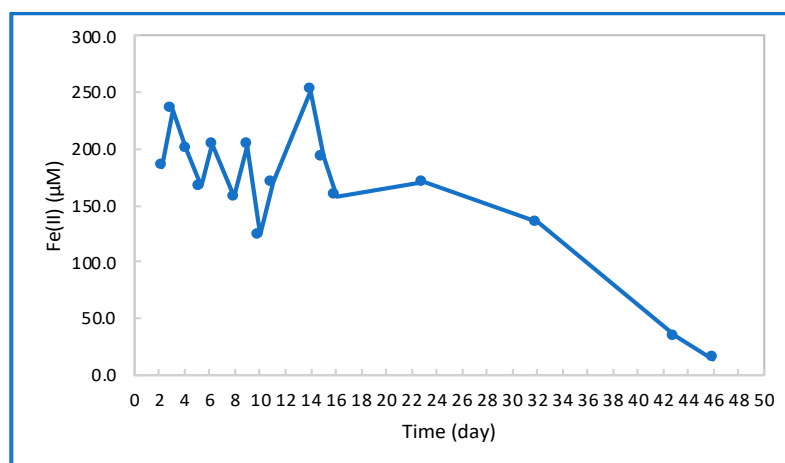


Figure 7. Occurrence of Fe(II) and variation in Fe(II) level over time during the floating Fe(III) film formation observed in the Second Test of Case Study (April–May 2023).

Figure 7 shows important, interesting findings regarding the film phenomenon and its mechanism. First, Fe(II) indeed appeared as detected, which verifies the occurrence and role of Fe(II) in the film formation. Second, the Fe(II) generated was sustained at a certain level (fluctuating around ~ 170 μM for ~ 2 weeks), for a prolonged period (over 3 weeks), although the experimental setup was open to air (O_2). Third, the Fe(II) level gradually started to drop after ~ 3 weeks, and eventually, the Fe(II) appeared to fade away after ~ 6 weeks. These findings are consistent with those of Roden and Urrutia [57].

The Fe(II) we found was approximately ~ 200 μM (0.2 mM), comparable, in order of magnitude, to the 3–5 mM found for the Tennessee and North Carolina soils [57]. The Fe(II) level in our study (~ 0.2 mM or ~ 11.2 mg/L) is also comparable to the levels of 0.53–19.8 mg/L seen in the associated waters collected in situ, where naturally occurring Fe(III) films were collected [39]. Occurrence of and increase in Fe(II) are quite typical of water-logged or inundated soils after being freshly flooded [35].

Our Fe(II) study provided useful information and experimental evidence regarding the mechanistic picture of Fe(III) film formation. It is notable that the Fe(II) generation was indeed mediated by the anaerobic microbes, and the Fe(II) level was kept microbially as well (steps R2 and P2 in Figure 5). It was only when the sugar was finally used up that the microbes ceased to function, which led to the slowing down and eventual halt of Fe(II) generation. This chain of events then tipped the seesaw of the Fe(III)/Fe(II) couple from Fe(II) to Fe(III), since in the absence of the microbial control of DO level to be anaerobically favorable, the Fe(II) present would all be oxidized to Fe(III) while no more Fe(II) then was generated.

It needs to be mentioned that the Fe(III) film layer itself could help to cut the O_2 and thus benefit the sustained existence of the Fe(II). The observed fluctuation in Fe(II) level could be partially due to the inevitable opening of the Fe(III) film layer upon sampling of the Fe(II) in the solution beneath the Fe(III) film layer. The Fe(II) fluctuation could also be indicative of the fluctuation in anaerobic activities.

It needs to be pointed out that sampling the Fe(II) in the solution beneath the films covering the solution surface can be quite challenging. Among other things, we noticed that the solution sampled may not be clear, since the system was a submerged soil with suspended particles; the sampling operation (use of a dropper or pipet) could disturb the solution. As such, the complications could pose difficulty to direct spectrophotometric analysis of the Fe(II) in the samples taken. The sampling error (uncertainty) could thus overwhelm the analytical error involved in the entire sampling and analysis of the Fe(II). Nevertheless, a useful peek at the Fe(II) generated during the Fe(III) film formation and transformation did successfully stem from this Fe(II) study. This work provides valuable experiences for further study to probe the generation and status of Fe(II) during Fe(III) film formation and transformation.

Abiotic Fe(III) film generation using Fe(II) salt: To further study the role of Fe(II) in floating Fe(III) film formation, we conducted some simulation tests to demonstrate the formation of the films under abiotic conditions as a result of oxidation of the ferrous Fe (Fe(II)) directly added to the systems, as compared to the Fe(II) from microbial reduction of the Fe(III) species in microbially mediated Fe(III) film formation. All eleven simulation tests (Tables 4–6) delivered floating thin films, regardless of how the various simulations were carried out (e.g., with a sand top (S1) in Figure 8, or without a sand top (S2)) and how the treatments were varied, with the amount and size of the films varying from test to test.

Both control tests (CT-GZ1, CT-GZ2, Table 6) gave no trace of any films. It is notable that the appearance, thickness, and morphology of the films closely resemble those for the films occurring naturally in the field and on the water surface of the tested fresh soils in our laboratory setting, as seen previously in Figures 2 and 3. These results demonstrate that the floating films observed in the abiotic simulation tests are indeed composed of the insoluble Fe(III) species that originate from oxidation of the soluble Fe(II) salt added. This notion is reinforced by the positive results of two S3 tests (Table 6) in which the Fe(II) salt alone without sand added to mimic the soil system still yielded some floating films.

The effect of the quantity of water and Fe(II) was studied. The effect of the water amount is twofold: (a) higher Fe(II) concentration as a result of less water and (b) shorter Fe(II) diffusion path to water surface (shorter water depth). These may jointly contribute to more films seen for S1-KS4 (Figure 8d) than S1-KS1 (Figure 8a). The S1 and S2 tests show that water depth appears to be a notable factor in film formation. The S1 tests with a higher water level (60 mL) and a higher overall Fe(II) concentration (Table 4) apparently yielded thinner or less visible films (Figure 8a), while the S2 tests with a lower water level (40 mL) and a lower overall Fe(II) concentration (Table 5) appeared to show more pronounced film formation. This seems to suggest that water depth appears to be a more effective factor than the overall Fe(II) concentration. It is likely that there might be sufficient Fe(II) in the systems already to generate Fe(III) films for all the treatments, which thus appears to leave water depth as a deciding factor.

It appears that beaker coverage made no apparent difference to film formation. This may be because there was sufficient O₂ in the headspace above the covered solution for Fe(II) oxidation since the thin films only need very small amounts of O₂ as well as Fe(III) to form. In addition, the plastic sheet cover may not completely have cut the supply of O₂ from the air since these thin plastic sheets are probably also O₂-permeable, as they are known to be moisture-permeable although the permeation is slow.

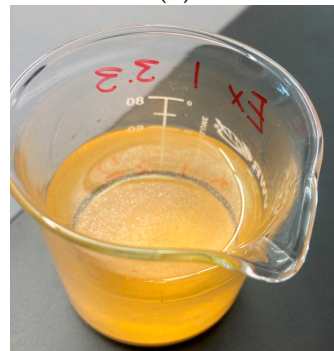
It seems that the treatments without N₂ purging (e.g., S2-GZ8, S2-GZ9) and those without the beakers being sealed (e.g., S1-KS2, S2-GZ7, S2-GZ9) led to fewer films. This may be due to more Fe(II) having been oxidized in the presence of more DO as a result of no purging or no seal; more insoluble Fe(III) can lead to more precipitation of hydrolyzed Fe(III) species settled out to the beaker bottom. The same is true for the Fe(II)-only tests (Table 6) in which S3-GC11 had more insoluble Fe(III) settled than S2-GC10.



(a)



(b)



(c)



(d)

Figure 8. Results of the simulation experiments for abiotic Fe(III) film generation using Fe(II) salt and water. All eleven simulation treatments yielded floating Fe(III) films, as shown for (a) test S1–KS1 (treatment: 60 mL deoxygenated H₂O/sand/Fe(II)/beaker covered), (b) test S1–KS2 (treatment: 60 mL deoxygenated H₂O/sand/Fe(II)/no cover), (c) test S2–KS3 (treatment: 60 mL deoxygenated H₂O/sand/Fe(II)/beaker covered/no extra sand layer), and (d) test S1–KS4 (treatment: 40 mL deoxygenated H₂O/sand/Fe(II)/beaker covered).

Interestingly, the floating films in the tests with sealed beakers remained thin and colorless over days, while the films in the fresh soil tests with open beakers changed to

thicker orange films and eventually to thick orange-red/red crusts. This seems to suggest the role O_2 played in the transformation of the films over time.

The mechanistic process of the artificial abiotic generation of the floating Fe(III) films using the simulation systems surely warrants further investigation to fully understand the formation of floating Fe(III) films under the circumstances of our simulation study. The most significant outcome of this simulation study is the actual occurrence of floating Fe(III) films delivered by abiotic simulations and the verification of the films being Fe(III) species. These studies provided valuable experiences as well as insights and thus pave the way for further sophisticated investigations.

3.6. Transformation, Growth, and Aging of the Floating Fe(III) Films: A Polymeric Model

To account for the transformation of the Fe(III) films that encompass various stages of compositional and structural changes over the entire span from their initial formation to subsequent transformation, growth, and aging, we created a polymeric model in terms of Fe(III) polymer development.

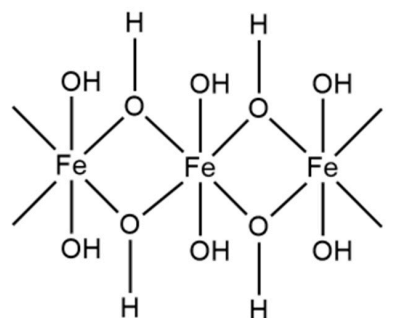
General considerations for the Fe(III) film transformation model: This polymeric model considers the presence of only Fe(III) species and water in the system without the potential effect of companion anions, especially organic ligands including natural ligands such as humic substances (fulvic acids, FA; humic acids, HA) and small molecular mass organic acid ligands such as acetate, oxalate, pyruvate, citrate, etc. (some generated from microbial metabolism). Hence, the only processes considered are the Fe(III) hydrolysis and polymerization of various Fe(III) hydrolysis products in the aqueous system.

This Fe(III) film transformation model has a group of major fundamental features:

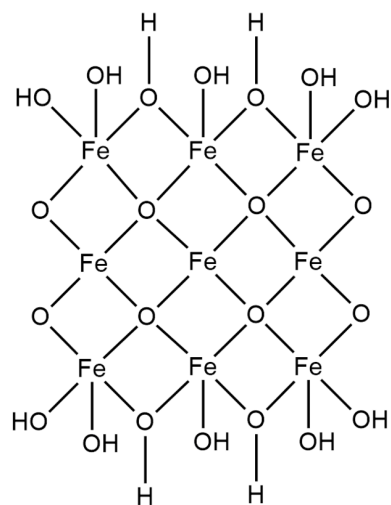
- (1) Fresh monomers of various Fe(III) hydrolysis products are unstable in an aqueous medium and stabilize by polymerization to form various more condensed assemblies of Fe(III) polymers. All of the various Fe(III) hydrolysis products (i.e., $Fe(OH)^{2+}$, $Fe(OH)_2^+$, and $Fe(OH)_3$) polymerize to form various more stable Fe(III) polymers.
- (2) The various Fe(III) hydrolysis products eventually form various kinds of polymers of well-defined structures and compositions from dimers to Fe_2O_3 . First, the hydrolysis products form dimers and trimers and, subsequently, linear polymers with multi-Fe(III) present; linear Fe(III) polymers then form 2D polymer sheets, and the polymer sheets form 3D Fe(III) assemblies to ultimately become Fe_2O_3 .
- (3) Various intermediate and incomplete Fe(III) polymers can occur over the entire span of formation and transformation of the various Fe(III) polymers.
- (4) All the various dimers, trimers, linear chain polymers, 2D polymer sheets, and 3D polymer assemblies of various Fe(III) hydrolysis products form following a single, fundamental mechanism: condensation polymerization via H_2O elimination. Hence, the entire polymerization process involving various Fe(III) hydrolysis products can essentially be viewed as a chemical process of dehydration.
- (5) Floating Fe(III) films, from small patches to very thin colorless films with reflective rainbow irradiance to colored thicker films to final orange/orange-red thick crusts, are essentially composed of the various Fe(III) polymers in complete, intermediate, and incomplete polymeric forms from linear Fe(III) polymers to 2D Fe(III) polymer sheets to 3D Fe(III) polymer assemblies.
- (6) Fe(III) film polymers in initial or early stages of formation may still be structurally amorphous and not amendable to X-ray diffraction detection. Hence, identification and verification of the various Fe(III) polymers representing floating Fe(III) films in various stages of formation, transformation, and aging from linear polymers to their final 3D forms can be challenging and thus would require enlisting of the various direct and indirect technical means available.

Our model for Fe(III) film transformation features three representative polymer schemes: (I) the 2D $Fe(OH)_3$ polymer sheet (Figure 9a), (II) the 2-D $FeOOH$ polymer sheet (Figure 9b), and (III) the 3D Fe_2O_3 assembly (Figure 9c). These Fe(III) polymer species

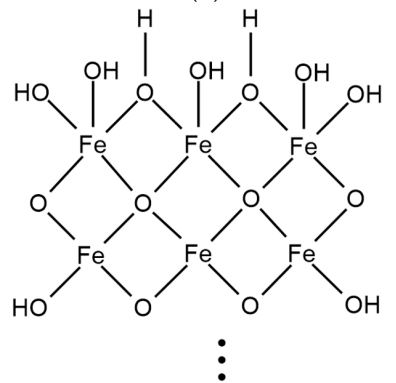
serve as landmarks in this polymeric model to depict the transformation of the Fe(III) films. Below, the formation of Fe(III) polymers for each scheme is described elaborately.



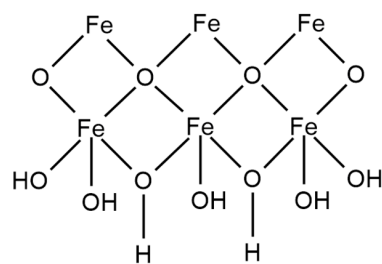
(a)



(b)



⋮



(c)

Figure 9. A schematic sketch of (a) the structures of the $\text{Fe}(\text{OH})_3$ polymer chain and the $\text{Fe}(\text{OH})_3$ polymer sheet, (b) the structure of the FeOOH polymer sheet, and (c) the structure of the Fe_2O_3 polymer,

proposed for the floating Fe(III) films. Note: The sketches are not shown exactly following the composition stoichiometry; only the top and bottom layers are shown for (c) and the interior of the Fe₂O₃ structure contains identical, repeating octahedral FeO₆ units joined by O sharing with Fe(III) as shown for the top and bottom layers. (b,c) each provide only a partial sketch of the Fe(III) polymer structures with some details left out as a result of the difficulty in showing the 3D structures with Fe(III) supposedly connected to six O ions (or OH groups at the edges and the top and bottom); only the sharing of O with Fe(III) is particularly shown to depict how Fe(III) connects to O to form the polymer structures.

Formation of linear Fe(OH)₃ polymer chains: These can form mechanistically through condensation of Fe(OH)₃ monomers, as shown in Figure 6, where a case of an Fe(III) dimer formation is depicted with respect to how the two monomers ([Fe(H₂O)₅(OH)]²⁺) form a dimer ([Fe(H₂O)₄(OH)₂Fe(H₂O)₄]⁴⁺) via elimination of two H₂O molecules.

Starting from the dimer described above, the Fe(III) polymers can then grow from a dimer to a trimer and eventually to a linear polymer chain, as shown in Figure 9a, for the connection between Fe and O in the polymer chain, following the identical mechanism. This growth of the linear Fe(III) polymer proceeds on both ends of the dimer or a polymer chain segment. This polymer chain development exemplifies a typical case of linear polymerization (e.g., formation of polyethylene: $n\text{H}_2\text{C}=\text{CH}_2 \rightarrow \{-\text{H}_2\text{C}-\text{CH}_2-\}_n$).

Fe(OH)₃ polymer sheet formation (Scheme 1): Following the identical mechanism (Figure 6), the Fe(OH)₃ polymer chains can condense together not only at the ends but also on the sides of the polymer chains and eventually on the sides of the polymer sheet after the Fe(OH)₃ polymer grows to a 2D sheet. This sideways polymerization yields a 2D Fe(OH)₃ polymer sheet, as depicted schematically in Figure 9a. Figure 10 presents a ball-stick model to show the Fe(OH)₃ polymer sheet from various perspectives (overview, top view, side view).

Ball-Stick Models for Octahedral FeO₆ Unit and Part of Fe(OH)₃ Polymer Sheet Composed of FeO₆ Units

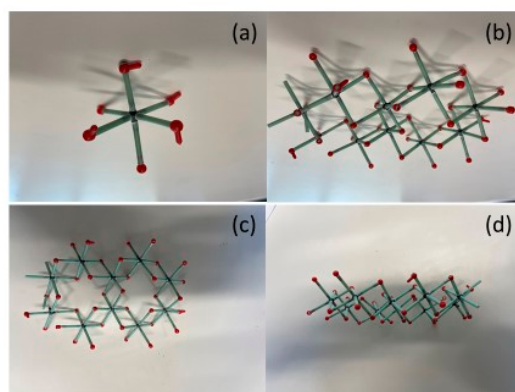


Figure 10. A presentation of the ball-stick models for (a) a single octahedral FeO₆ unit with three O atoms in one plain staying on the surface and the other three in another plain above the surface, (b) an overview of part of an Fe(OH)₃ polymer sheet, (c) a top view of part of an Fe(OH)₃ polymer sheet, and (d) a side view of part of an Fe(OH)₃ polymer sheet. Note: O is in red; Fe(III) is in the center of the Fe(III)O₆ units without the Fe(III) being recognizably shown in color.

The fusing of Fe(III) from two Fe(III) polymer chains proceeds through edge-sharing of the Fe(III)O₆ octahedral units (Figures 9a and 10). This picture is consistent with the structural consideration of the Fe(III) polymers (Fe_pO_r(OH)_s^{3p - (2r + s)}, where $p = 2$ for dimer, $p = 3$ for trimer) suggested by Schneider and Schwyn [11]. The general bridging positions of the Fe(III) polymers for connecting the Fe³⁺ ions are occupied solely by OH⁻ (or by O²⁻ and OH⁻ for the polymers of more complex structures not depicted here) [11].

The $\text{Fe}(\text{OH})_3$ polymer sheet can also form by fusing of individual $\text{Fe}(\text{III})$ monomers, dimers, and trimers separately to an $\text{Fe}(\text{OH})_3$ polymer chain or a sheet via condensation.

Fe(OH)₃ polymer sheet structure: This polymer sheet is composed of many octahedral $\text{Fe}(\text{III})\text{O}_6$ units (see Figure 6 for the octahedral structure) with O bridging the $\text{Fe}(\text{III})$ ions by sharing of O with $\text{Fe}(\text{III})$. In the 2D sheet, each octahedral $\text{Fe}(\text{III})\text{O}_6$ unit stays in the sheet plain in the way with three O anions at the plain bottom and the other three at its top in between the two O anions at the bottom plain (Figures 6b and 10a, Table 11).

Table 11. Charge balance and composition formula for the $\text{Fe}(\text{OH})_3$ polymer composed of $\text{Fe}(\text{III})\text{O}_6$ units.

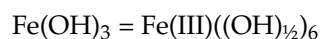
Polymer	Fe(III)–O Connection and O Sharing	Charge Balance	Structure	Composition Formula
$\text{Fe}(\text{OH})_3$	Each O shares with 2Fe(III)	(i) O shares with 2Fe(III), for each O, -1 used to balance Fe(III), each O gives $(-1)/2 = -1/2$ charge to Fe(III) (remaining -1 balanced by H^+ to form OH); (ii) 6O in $\text{Fe}(\text{III})\text{O}_6$ with each O giving $-1/2$ charge to Fe(III), so total O charge = $(-1/2) \times 6 = -3$ to balance $+3$ of Fe(III)	(i) Each O shares with 2Fe(III), each O gives $1/2\text{O}$ (i.e., $1/2\text{OH}$) to Fe(III); (ii) Total OH connected to Fe(III) in $\text{Fe}(\text{III})\text{O}_6$: $(1/2)\text{OH} \times 6 = 3\text{OH}$, so that $\text{Fe}(\text{III})\text{:OH} = 1\text{:}3$	$\text{Fe}(\text{III})\text{:OH} = 1\text{:}3 \rightarrow \text{Fe}(\text{OH})_3$

Charge balance for Fe(OH)₃ polymer sheet: In the 2D $\text{Fe}(\text{III})$ polymer sheet, each O shares with two $\text{Fe}(\text{III})$ ions to construct the connected (polymerized) sheet structure. Each O has a total of two negative charges (-2), which needs to satisfy the charge balance for a total of three positive charges ($+3$) owned by one central $\text{Fe}(\text{III})$. Since each O is shared by two central $\text{Fe}(\text{III})$ cations, one half of the negative charge ($-1/2$) from one O is used to balance the positive charge of the $\text{Fe}(\text{III})$. Each central $\text{Fe}(\text{III})$ has six O anions around it in the octahedral $\text{Fe}(\text{III})\text{O}_6$ unit and thus the total of the negative charge from all the six charge-contributing O anions around the $\text{Fe}(\text{III})$ is $(-1/2) \times 6 = -3$, which balances the $+3$ charge of the central $\text{Fe}(\text{III})$ (Table 11).

The remaining one negative charge (-1) left unused from each O anion will then be balanced by one H^+ cation each with one positive charge ($+1$) to form an OH group. Hence, each and every one of the O anions on both the top and bottom plains of the 2D $\text{Fe}(\text{OH})_3$ polymer sheet has one H^+ attached to become one OH to satisfy the overall charge balance for the O anions. Thus, the 2D polymer sheet has OH groups on both of its top and bottom plains. For each O^{2-} ion, since each O shares with two $\text{Fe}(\text{III})$ ions, its charge balance is summarized as follows: $(-1/2)$ to $\text{Fe}(\text{III}) + (-1/2)$ to $\text{Fe}(\text{III}) + (-1)$ to H^+ (Table 11).

Composition formula of Fe(OH)₃ polymer sheet corresponding to its structure: Each central $\text{Fe}(\text{III})$ connects to six OH groups (three at the sheet top and three at the bottom) with only a half of one OH owned by each $\text{Fe}(\text{III})$ as a result of the sharing of the OH by two $\text{Fe}(\text{III})$ ions in two octahedral $\text{Fe}(\text{III})\text{O}_6$ units. Hence, the total number of OH groups owned by one central $\text{Fe}(\text{III})$ is $\{(1/2)(\text{OH})\} \times 6 = 3\text{OH}$ groups (i.e., $\text{Fe}(\text{III})\text{:OH} = 1\text{:}3$). This well fits the composition formula for the 2D $\text{Fe}(\text{OH})_3$ polymer sheet (Table 11).

Interestingly, the octahedral connection of the central $\text{Fe}(\text{III})$ with the six OH groups around it and the sharing of the O (actually O–H or OH) with the $\text{Fe}(\text{III})$ in the $\text{Fe}(\text{OH})_3$ polymer are actually embedded in the very composition formula of $\text{Fe}(\text{OH})_3$:



At the edges of the $\text{Fe}(\text{OH})_3$ polymer sheet, no more $\text{Fe}(\text{III})$ is available to share the edge O anions (broken bonds for edge O anions), and then the remaining one negative charge (which would be balanced collectively by two $\text{Fe}(\text{III})$ ions) will be balanced by one

H⁺ ion. Hence, the edges of the 2D Fe(OH)₃ polymer sheet are composed of OH groups as well (much like the bottom and top of the polymer sheet).

A distinct structural feature of the Fe(OH)₃ polymer sheet is that it bears a polymer that contains only one layer of Fe(III) between the two layers of OH groups sandwiched around the middle Fe(III) layer, with one OH layer above the Fe(III) layer and one OH layer below (Figure 9a). This Fe(III) polymer sheet structure resembles the Al(III) polymer sheet present in soil clay minerals [20,83–85]. It is thus conjectured that the initial colorless (very) thin films with the characteristic reflective rainbow iridescence likely may bear the structure of the 2D Fe(III) polymer sheet shown in Figure 9a.

FeOOH polymer formation (Scheme II): The 2D Fe(III) polymer sheets (i.e., Fe(OH)₃ polymer sheets, Figure 9a) can continue to grow, via the polymerization through H₂O elimination, to form thicker sheets with more layers of Fe(III) built in (or fused in) (Figure 9b) as compared to the Fe(OH)₃ sheet that has only one layer of Fe(III) (Figure 9a). A new Fe(III) polymer of such a kind can form, for example, by fusing of two more single one-Fe(III)-layer Fe(OH)₃ sheets (Figure 9a) to another single one-Fe(III)-layer Fe(OH)₃ sheet (Figure 9a), one on its top and the other on its bottom, to yield an Fe(III) polymer with three layers of Fe(III), i.e., the FeOOH polymer shown in Figure 9b.

FeOOH polymer structure: Three 2D Fe(OH)₃ polymer sheets (Figure 9a) join (fuse) together to form one FeOOH sheet through the corner-sharing of the Fe(III)O₆ octahedral units (Figure 9b). Upon the connection (fusing) of the three individual Fe(OH)₃ polymer sheets, one Fe(OH)₃ sheet is positioned between the two other Fe(OH)₃ sheets; the top layer of the OH groups of the middle single Fe(OH)₃ sheet join the bottom layer of the OH groups of another single Fe(III) sheet above the middle Fe(III) sheet and thus fuse together by sharing O between the two layers of Fe(III) from each individual Fe(OH)₃ sheet after elimination of one water molecule from the two OH groups. In this elimination, one H from one OH group of one Fe(III) sheet and one entire OH from the OH group of another Fe(III) sheet are eliminated as one H–OH, and the remaining O in the OH group, after its H is eliminated, then connects the two Fe(III) ions from the two Fe(III) sheets.

To complete the formation of one FeOOH polymer sheet, an identical connection of the middle Fe(OH)₃ sheet with another Fe(OH)₃ sheet below the middle Fe(OH)₃ sheet occurs via the same elimination of the OH groups from the two Fe(OH)₃ sheets, and this time, the bottom layer of the OH groups of the middle Fe(III) sheet fuse with the top layer of the OH groups of the Fe(OH)₃ sheet below the middle Fe(OH)₃ sheet (Table 12).

The FeOOH polymer sheet can also form by fusing of single, individual Fe(OH)₃ monomers and/or Fe(III) dimers and trimers, or segments of the Fe(OH)₃ polymer sheets and chains to one Fe(OH)₃ polymer sheet, simultaneously, or separately.

In summary, the newly formed FeOOH polymer (Figure 9b, Table 12) has three layers of Fe(III) (from the three original individual Fe(OH)₃ sheets). The middle Fe(III) layer of the FeOOH polymer on its top connects to the Fe(III) layer of another Fe(OH)₃ sheet above through the O shared between these two Fe(III) layers (Figure 9b). Likewise, the middle Fe(III) layer on its bottom connects to the Fe(III) layer of another Fe(OH)₃ sheet below (Figure 9b).

Hence, overall, one FeOOH polymer has a total of seven layers: from top to bottom sequentially, (i) OH layer, (ii) Fe(III) layer, (iii) shared O layer, (iv) Fe(III) layer, (v) shared O layer, (vi) Fe(III) layer, and (vii) OH layer. Hence, in total, numerically, one such an FeOOH polymer sheet thus contains two OH layers (one at top, one at bottom), two shared O layers (fusing Fe(III) together), and three Fe(III) layers (Figure 9b).

Charge balance for FeOOH polymer: This FeOOH polymer contains three layers of Fe(III): one layer of Fe(III) at the top and, symmetrically, one layer of Fe(III) at the bottom, with one Fe(III) layer in the middle of the top and bottom Fe(III) layers (Figure 9b). To find out the charge balance, we consider three single Fe(III) ions in an FeOOH polymer, one Fe(III) in the middle layer (the middle Fe(III)), one at the bottom (the bottom Fe(III)), and the other at the top (the top Fe(III)) (Figure 9b, Table 12).

Table 12. Charge balance and composition formula for the FeOOH polymer composed of Fe(III)O₆ units.

Polymer	Fe(III)–O Connection and O Sharing	Charge Balance	Structure	Composition Formula
FeOOH	(i) Three Fe(III): top, middle, and bottom; (ii) Top Fe(III): each of 3O on top side of Fe(III)O ₆ shares with 2Fe(III), each of 3O on bottom side of Fe(III)O ₆ shares with 4Fe(III); (iii) Middle Fe(III): each O shares with 4Fe(III); (iv) Bottom Fe(III): each of 3O on top side of Fe(III)O ₆ shares with 4Fe(III), each of 3O on bottom side of Fe(III)O ₆ shares with 2Fe(III)	(i) For O sharing with 2Fe(III), each O gives $(-1)/2 = -1/2$ charge to Fe(III) (remaining -1 balanced by H ⁺ to form OH); (ii) For O sharing with 4Fe(III), each O gives $(-2)/4 = -1/2$ charge to Fe(III); (iii) Top Fe(III): 3O with each O sharing with 2Fe(III) plus 3O with each O sharing with 4Fe(III), total O charge = $(-1/2) \times 3 + (-1/2) \times 3 = -3$ to balance +3 of Fe(III); (iv) Middle Fe(III): 6O with each sharing with 4Fe(III), total O charge = $(-1/2) \times 6 = -3$ to balance +3 of Fe(III); (v) Bottom Fe(III): same as top Fe(III)	(i) Top Fe(III): 3OH each sharing with 2Fe(III) plus 3O each sharing with 4Fe(III), so top Fe(III) has $(1/2)OH \times 3 + (1/4)O \times 3$; (ii) Middle Fe(III): 6O each sharing with 4Fe(III), so middle Fe(III) has $(1/4) \times 6O$; (iii) Bottom Fe(III): same as top Fe(III), so each Fe(III) has $(1/4)O \times 3 + (1/2)OH \times 3$ (iv) Total O for 3Fe(III): $(1/4) \times 3 + (1/4) \times 6 + (1/4) \times 3 = 3O$, total OH for 3Fe(III): $(1/2) \times 3 + (1/2) \times 3 = 3OH$, so 3Fe(III):3O:3OH	Fe(III):O:OH = 1:1:1 → FeOOH

For the middle Fe(III) (Figure 9b), since each O shares with four Fe(III) ions, each Fe(III) gets one quarter of the -2 charge of one O shared with the four Fe(III) ions, which then means $(-2) \times (1/4) = -1/2$ charge from one O contributing to one Fe(III). Since each Fe(III) in its Fe(III)O₆ unit has six O ions around it, the total negative charge from the six shared O ions is $(-1/2) \times 6 = -3$, balancing the +3 charge of the central Fe(III) in the Fe(III)O₆ unit (Table 12).

Now, for the top and bottom Fe(III) ions considered (Figure 9b), each Fe(III) in its Fe(III)O₆ unit has two sides of O anions. One side of the octahedral unit has three O anions shared with the middle Fe(III) and the other side of the unit has three OH groups, i.e., O connected to one H⁺ for charge balance, rather than connected to (shared with) Fe(III).

Hence, for the top and bottom Fe(III), each of the three O anions shared with the middle Fe(III) is shared with four Fe(III) ions, identical to the case of the middle layer Fe(III). Each of these three O anions thus gives $-1/2$ charge to the Fe(III), i.e., $(-2)/4 = -(1/2)$ (Table 12).

For the OH groups of the top and bottom Fe(III), these are similar to what exists at the top and bottom of the Fe(OH)₃ polymer sheet (Figure 9a). Each O of the OH group is thus connected with only two Fe(III) ions (rather than four Fe(III) ions like for the middle layer Fe(III)). Consequently, each of the three O anions has its negative charge (-2) split to give one negative charge (-1) to the two Fe(III) equally shared and the other negative charge (-1) to be balanced by H⁺ as one OH group. Thus, each of these three O anions gives $-1/2$ charge (i.e., $(-1)/2 = -1/2$) to the Fe(III) in its Fe(III)O₆ unit (Table 12).

For the top and bottom Fe(III) alike, the charge balance scenario is as follows: Each O of the three O anions connected to the middle Fe(III) gives $-1/2$ (i.e., $(-2)/4$) charge to the Fe(III) in its Fe(III)O₆ unit, that is, $(-1/2) \times 3 = -3/2$. Each of the three O anions not connected to the middle Fe(III) on the other side (connected to H⁺ as OH group) also gives $-1/2$ (i.e., $(-1)/2$), that is, $(-1/2) \times 3 = -3/2$. Combining the total charge from the two groups of the O anions for one central Fe(III) in its Fe(III)O₆ unit for the top and bottom Fe(III) each then amounts to $(-3/2) + (-3/2) = -3$, which balances the +3 of the Fe(III) (Table 12).

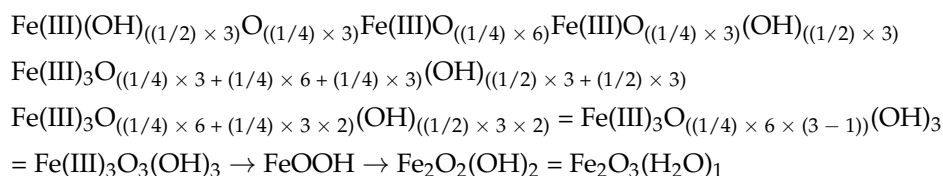
Composition formula of FeOOH polymer corresponding to its structure: For the middle Fe(III), it gets one quarter of one O anion since each O is shared with four Fe(III) ions and thus each Fe(III) gets $(1/4) \times 6O$ ions in total (Table 12).

For the top and bottom Fe(III) ions considered, each Fe(III) has three O ions each shared with four Fe(III) ions (i.e., $1/4O$ attributed to one Fe(III) from each O) and the other three O ions connected to H^+ as OH groups. However, each OH group is shared with only two Fe(III) ions and thus only a half OH group is attributed to one Fe(III) from each O.

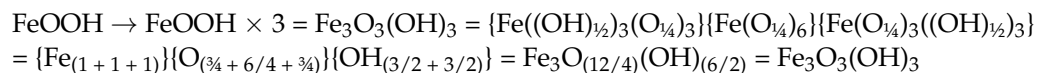
Hence, for the top and bottom Fe(III) ions, each Fe(III) gets $(1/4) \times 3O$ and $(1/2) \times 3OH$, and thus both top and bottom Fe(III) ions in combination have $(1/4) \times 3 + (1/4) \times 3 = (1/4) \times 6O$ anions and $(1/2) \times 3 + (1/2) \times 3 = (1/2) \times 6OH$ groups in total (Table 12).

Finally, for the total three Fe(III) ions (top, bottom, and middle) considered together, the total number of $(1/4) \times 6O$ connected to both the top and bottom Fe(III) ions plus the total number of $(1/4) \times 6O$ connected to the middle Fe(III) yields a total of $((1/4) \times 6) \times 2O = 3O$ for the three Fe(III) ions considered (i.e., Fe(III):O = 3:3). The OH groups connected to the top and bottom Fe(III) ions is $(1/2) \times 6(OH) = 3OH$ (i.e., Fe(III):OH = 3:3). Hence, collectively, the composition ratio obtained by counting the total O and OH connected to all the three Fe(III) ions considered thus gives rise to the following ratio: Fe(III):O:OH = 3:3:3, which is equivalent to the composition formula of FeOOH (Table 12).

The above derivation of the composition formula for the FeOOH polymer with three Fe(III) ions considered corresponding to three layers of Fe(III) can be summarized below:



The connection of the central Fe(III) with the surrounding O ions and OH groups and the sharing of the O anions and OH with the Fe(III) in FeOOH polymer are also implicitly given in the composition formula of FeOOH corresponding to its structure shown below:



The FeOOH polymer sheets (Figure 9b) are considered to be the intermediate thicker Fe(III) films. Probably, the same condensation process as described for the formation of the FeOOH polymer sheets can proceed further to generate various intermediate Fe(III) polymer sheets or polymers with more Fe(III) layers (more than three Fe(III) layers) by fusing of more Fe(OH)₃ polymer sheets or of individual Fe(III) monomers, dimers, trimers, and/or the Fe(OH)₃ polymer sheet segments. Yet, these intermediate polymers are still structurally unstable thermodynamically and eventually further transform to form stable Fe₂O₃ solids. This is actually a process of dehydration in consideration of the decrease in the amount of H and O in the Fe(III) polymers by condensation via water elimination.

Fe₂O₃ formation (Scheme III): In the subsequent further Fe(III) polymer development, the FeOOH polymers then grow to become Fe₂O₃ by joining the Fe(III) polymers (and also monomers, dimers, trimers, and/or polymer segments) to the FeOOH polymer sheet on both its top and bottom via the H₂O elimination reaction through corner-sharing of the Fe(III)O₆ units (i.e., fusing of more Fe(OH)₃ sheets to the FeOOH sheet at both its bottom and top) as shown in Figure 9c. This growth in Fe(III) layers by addition of more Fe(OH)₃ sheets will eventually lead to the formation solid Fe₂O₃, as shown in Figure 9c.

Charge balance for Fe₂O₃: Each O shares with four Fe(III) ions throughout the 3D Fe₂O₃ assembly, and thus only one-quarter of the O is available to each Fe(III) shared with the O. Hence, similarly, each O contributes a negative charge of $(-2) \times (1/4) = -1/2$ to one Fe(III). Since each central Fe(III) has six O ions around it, the total negative charge contributed

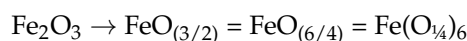
by all six O ions, each with $-1/2$ is $(-1/2) \times 6 = -3$, balances the $+3$ of the Fe(III) cation (Table 13).

Table 13. Charge balance and composition formula for Fe_2O_3 composed of Fe(III)O_6 units.

Polymer	Fe(III)–O Connection O Sharing	Charge Balance	Structure	Composition Formula
Fe_2O_3	Each O shares with 4Fe(III)	(i) Each O gives $(-2)/4 = -1/2$ charge to Fe(III); (ii) Total O charge: $(-1/2) \times 6 = -3$ to balance $+3$ of Fe(III)	(i) Each O gives $1/4$ O to Fe(III); (ii) 1Fe(III) in Fe(III)O_6 gets $(1/4) \times 6\text{O}$; (iii) Total O for 2Fe(III): $(1/4) \times 6 \times 2 = 3\text{O}$, so 2Fe(III):3O	Fe(III):O = 2:3 \rightarrow Fe_2O_3

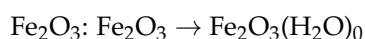
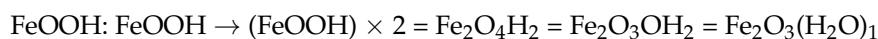
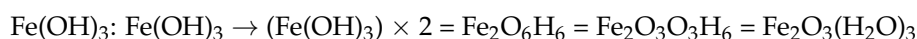
Composition formula of Fe_2O_3 corresponding to its structure: We consider two Fe(III) ions of Fe_2O_3 for the purpose of composition counting. Each O ion contributes one-quarter O to the central Fe(III). The total of O connected to one Fe(III) is $(1/4)\text{O} \times 6$. For the two Fe(III) ions considered, the total number of O amounts to $(1/4)\text{O} \times 6 \times 2 = 3\text{O}$. This is equivalent to the composition formula of Fe(III):O = 2:3 for the 3D Fe_2O_3 structure (Table 13).

Likewise, the octahedral link of the central Fe(III) with the O ions around it and the sharing of the O ions with the Fe(III) in the Fe(III)O_6 unit for Fe_2O_3 can also be revealed in the composition formula of Fe_2O_3 shown below:



Surfaces of Fe_2O_3 : All the OH groups on the edges, as well as the top and bottom of the Fe_2O_3 assembly (where exist broken bonds for O anions), can be ignored, and thus the H in the OH group on these broken surfaces is conventionally excluded in composition counting to arrive at the adopted composition formula of Fe_2O_3 . The treatment as such stems from the consideration that the amount of Fe(III) inside the Fe_2O_3 structure overwhelmingly surpasses that of the Fe(III) ions on the edges, top, and bottom of the Fe_2O_3 structure. This is why H does not appear in the composition formula of Fe_2O_3 , although the H in the OH group is indeed present at the edges (sides) and top and bottom of the Fe_2O_3 assembly. This is much like the case for polyethylene, with a polymer formula being $\{-\text{CH}_2-\text{CH}_2-\}_n$, in which the C atom at each of the two ends of the polymer chain should have one H to make up the broken bond to fulfil the four bonds required for each carbon. Yet, these two H atoms are ignored in the polymer formula.

Dehydration of Fe(III) polymers during their transformation: The Fe(III) polymers form and transform through polymerization via water elimination. Hence, the chain of polymerization events can essentially be viewed as a dehydration process. Interestingly, this feature is actually implicitly imbedded in the composition formulae for the Fe(III) polymers, such as Fe(OH)_3 , FeOOH , and Fe_2O_3 , as shown below:



Hence, the dehydration process along the polymerization can be described in one simple form: $\text{Fe}_2\text{O}_3(\text{H}_2\text{O})_3 \rightarrow 1 \rightarrow 0$. Furthermore, the three Fe(III) polymers of the Fe(III) films can be represented by a general composition formula, $\text{Fe}_2\text{O}_3(\text{H}_2\text{O})_n$ ($n = 3, 1, 0$), along the line of the polymeric model for the Fe(III) film polymer transformation. In consideration of the occurrence of various intermediate and incomplete Fe(III) polymers, as discussed before, this general formula can be modified to accommodate this consideration in the following form: $\text{Fe}_2\text{O}_3(\text{H}_2\text{O})_n$ ($n = 3-0$).

Our proposed structures of the floating Fe(III) films as various Fe(III) polymers across various stages of the continuous film transformation and growth appear to be consistent with the color variation in the films over time (see Figures 3 and 4, Tables 7 and 8).

Intermediate and incomplete Fe(III) polymers and polymer mixtures: When Fe(III) polymers transform from linear polymers to 2D sheets to 3D polymers, the Fe(III)O₆ units from various sources fused to the growing polymer structures do not have to be complete polymer chains or already-formed 2D sheets. The Fe(III) monomers and dimers and the segments of the linear Fe(III) polymers and 2D sheets can also further fuse to the growing polymers and yield intermediate and incomplete polymers. These partially completed polymer intermediates may look like the polymers with defects. These intermediate and incomplete polymers may well be part of the floating Fe(III) films.

Furthermore, the individual Fe(OH)₃ polymers with one layer of Fe(III) (Figure 9a) and the individual FeOOH polymers with three layers of Fe(III) (Figure 9b) can also join (not fuse) together to form polymer assemblies (not coherent new polymer structures, just thicker Fe(III) films) connected by hydrogen bonding. These mixture assemblies held by hydrogen bonding may also well be part of the floating Fe(III) films.

It is considered that the floating Fe(III) films consist of a wide range of the various Fe(III) polymers (both completely formed polymers and partially formed intermediates), including linear forms initially and 2D sheets with only one Fe(III) layer; subsequently, 3D polymer assemblies with a growing number of Fe(III) layers; and, eventually, 3D Fe₂O₃ colloids. The Fe(III) films actually find themselves in a complex mixture of all the various well-defined polymers embracing 1D, 2D, and 3D structures with a growing number of Fe(III) layers and also polymer assemblies of Fe(OH)₃ and/or FeOOH polymer sheets joined by H-bonding, together with various intermediates of all sorts.

Our preliminary calculations show that the densities of the proposed polymeric structures seem to be higher than that of water if all Fe(III) films assume these defined structures (e.g., as shown in Figure 9a,b). This finding is inconsistent with the fact that the Fe(III) films indeed float on water. This seems to suggest that the films are probably not composed solely of the proposed well-defined polymers. Instead, it is likely that the films actually formed probably exist as amorphous assemblies of small pieces of the proposed well-defined polymers, polymer segments, and intermediates with micropores filled in the assemblies (mixtures). The development of such assemblies may bear a fractal nature [86] in their morphology.

It is expected that the Fe(III) polymers in such complex mixtures as described above may fail to respond sensitively to various structural analysis techniques including X-ray diffraction analysis. The intermediate and incomplete Fe(III) polymers with defects are likely partially responsible for the amorphous nature of the amorphous Fe(III) polymers. Yet, the absence of X-ray diffraction signals may not necessarily prescribe the absence of these amorphous Fe(III) polymers. New experimental detection and verification of the various Fe(III) polymers, polymer intermediates, and mixtures in floating Fe(III) films thus warrant considerable attention in future research.

3.7. Formation and Transformation of the Floating Fe(III) Films in Real Environments

In natural soils and waters, many companion ions and molecules (ligands) are widely present. These can mediate and interfere with the formation and transformation of the Fe(III) films. Hence, the natural formation of the Fe(III) films in the field may proceed via different routes, possibly with different Fe(III) polymers generated. Recent studies on floating Fe(III) films [37–40] have also evidently pointed to this notion. Yet, it needs to be pointed out that although various ligands and other factors may interfere with the Fe(III) film formation and transformation, the fact remains that the floating Fe(III) films described in this paper and other studies indeed occur in the field and in laboratory settings where the ligands and other structures are inevitably present.

Effect of organic acids and ligands on Fe(III) film formation: Natural organic matter (NOM) plays a prominent role in floating Fe(III) film formation, especially considering

that NOM may act as organic ligands for Fe(III), which can increase the solubility of Fe(III) species and in turn impede or inhibit the film formation [37]. A study in which a prolonged test through artificial synthesis and abiotic generation of Fe(III) films showed that organic acids such as natural organic substances (humic acids and their photochemical-degraded products) played a decisive role in the final success of artificial, abiotic generation of the Fe(III) films that visually resemble the natural floating Fe(III) films observed in the field (the modified UVB method); addition of humic acids in the synthetic generation led to the Fe(III) films that best resembled the natural films [39]. This further reinforces the notion that floating Fe(III) films can only form under certain favorable conditions, depending on the film formation mechanism and on the source of Fe(II) in the specific systems, e.g., light-induced reduction of Fe(III)–NOM coordination compounds near or at the water surface, or discharged groundwater enriched with Fe(II) [37].

Our study appears to support the above discovery, since our setting also had organic materials and humic substances usually present in soils as a result of our usage of fresh, natural, living soils to deliver floating Fe(III) films. In our study, glucose was added, which led to the occurrence of fermentation. Hence, the organic acids (e.g., pyruvate and acetate) generated during fermentation, as well as the initial aerobic respiration, may also play a role in the formation of the Fe(III) films in our experimental setting.

Our latest study showed that oxalate ($C_2O_4^{2-}$, $^-OOC-COO^-$) and acetate (H_3CCOO^-) were able to interfere with Fe(III) film formation, while oxalate had a stronger effect than acetate; their effect depended on their levels present in the soil systems. As a well-known organic ligand, oxalate can form strong coordination compounds with Fe(III) to make Fe(III) more soluble and thus affect Fe(III) hydrolysis and the formation and growth of Fe(III) polymers and films. Humic acids were found to bind to Fe(III), as demonstrated by a water chemistry analysis using Visual MINTEQ 3.1 and the Stockholm Humic Model, and thus impede Fe(III) hydrolysis, and in turn interfere with the polymerization of the Fe(III) hydrolysis products [39].

Previous findings [39] and our results above collectively point to the essence of the natural formation of floating Fe(III) films, i.e., a slow, gradual, well-controlled pace for film formation, especially the Fe(III) supply and the formation of the initial films featuring an appearance like transparent thin plastic films. A fast supply of large amounts of Fe(III) can cause flocculation and precipitation of Fe(III), which can derail Fe(III) film formation. These organic substances may play a special role in mediating the special, specific pace favorable for the Fe(III) film formation. This special feature may be responsible for the success of the modified UVB method for the laboratory synthesis of the Fe(III) films [39]. This notion stems from the following novel interpretation of the role played by organic substances in the formation of the Fe(III) films: On the one hand, these various organic substances can make Fe(III) soluble, thus apparently impeding Fe(III) film formation. On the other hand, however, this Fe(III) solubility mediation exerted by organic substances can also control the level of Fe(III) available for its hydrolysis and thus secure and sustain the special pace favorable for the Fe(III) film formation without Fe(III) flocculation.

Sunlight and photochemical redox cycling of Fe(III)/Fe(II) facilitated by NOM can mediate the Fe(III) film formation. In our study, the only light was fluorescent light far above from the ceiling, which was very weak and thus could not exert significant photochemical mediation over the Fe(III) film formation [37,40].

Composition of the Fe(III) films: The Fe(III) films were found to be 87% in total Fe, and Si was the second most abundant [40], which is consistent with the finding of another study [39] in which Si was also found in the Fe(III) films tested (11–22%), and the Si was considered part of the film structure. It is interesting how Si (commonly present in soil clay minerals) got into the film structures, since the films are formed on the water surface, presumably as a result of soluble Fe(II) transport. It is especially curious that the films were successfully synthesized in the absence of Si in that study ([39]). The possibility might not be ruled out that the Si found might not actually exist within the Fe(III) film assemblies, but rather bear some other origin (e.g., brought in during film sampling, or tiny clay particles

mixed with the films, or some Si adsorbed on the films in some forms). Silica was also found in the Fe(III) films in another study [38]. It is of interest to explore if the Fe(III) films formed in our experimental laboratory setting would contain any silica.

Morphology of the Fe(III) films: The imaging results of the SEM (scanning electronic microscope) show that the Fe(III) films tested were platy in morphology without clear or with little topography, and cracking was found, apparently as a result of film dehydration [39]. The films initially floating on water in our study were not platy, but instead, very thin, continuous, and even somewhat transparent (Figure 3a), like plastic films (the initial thin films are very difficult to show using ordinary pictures, but clearly, decisively visible to the eyes). This suggests that the initial very thin films might bear some different Fe(III) hydroxide or oxyhydroxide structures as compared to the platy films (Figures 2 and 3b) and cracking films (Figures 3c and 4) that occurred in the later stages of the film formation in our study.

Structure of the Fe(III) films: Some Fe(III) films were found to be nanocrystalline, and the artificially synthesized films in the absence of organic matter exhibited higher degrees of structural order and crystallinity [39]. This provides some support for our polymeric model to account for the structures of the Fe(III) films. The insights gained from our study suggest that the structural difference for the naturally occurring Fe(III) films may stem from the mechanistic picture that natural film formation actually involves a slow, gradual microbial reduction of Fe(III) to Fe(II) followed by a slow, diffusive transport of Fe(II) to water surface with a subsequent steady oxidation of Fe(II) at the water surface by O₂ across an O₂ gradient at the water/air interface.

The natural formation of the Fe(III) films may differ from their synthetic generation, in which the Fe(II) salt was presumably well mixed in the container and thus there was a lack of a slow supply of Fe(II) to the water surface to secure a slow, gradual formation of the polymerizable Fe(III) hydrolysis products from a slow appearance of Fe(III) mandated by slow oxidation of the Fe(II) generated. It is considered that this slow process, as the hallmark of the natural floating film formation, is therefore responsible for the distinct characteristics of natural Fe(III) films, as reported in this paper.

Ferrihydrite as one of the major Fe(III) species in Fe(III) films: The ratio of Fe(II):Fe(III) in the Fe(III) films tested in a study was found to be 0.02–0.23 (mean: 0.14), which indicates that Fe(III) films are predominantly Fe(III) in composition [39]. It remains uncertain whether the slight amount of the Fe(II) detected in the films was within the Fe(III) polymeric structures of the films, adsorbed on the surfaces of the films, or perhaps associated with the organic materials attached to the films.

The Fe(III) films from the water of ephemeral pools with a discharge of Fe(II)-rich groundwater on sand deposits were found to exhibit hydroxides of both Fe(II) and Fe(III) in a Fe(II):Fe(III) ratio of 1:3, and Fe(III) hydroxides were considered to be the precursors for two-line ferrihydrite [38]. This supports our polymeric model for the transformation of the Fe(III) films. Spectroscopic results (i.e., transmission electron microscopy (TEM), electron energy loss spectrometry (EELS), scanning electron microscopy (SEM), and X-ray diffraction (XRD)) show that the natural Fe(III) films bear nanocrystalline structures of ferrihydrite [39]. This is supported by the finding of another study in which the X-ray diffraction data also point to the presence of two-line ferrihydrite in films from field and laboratory culture samples [40].

The iron in floating films of natural waters in south-central Sweden was characterized by using extended X-ray absorption fine structure (EXAFS, a technique of synchrotron-based X-ray absorption spectroscopy (XAS)) [37]. It was found that in two groundwater discharge sampling locations, the only chemical component present in the film samples was ferrihydrite and the Fe···Fe distances were lower in the tested natural samples than in the synthesized ferrihydrite, indicative of a somewhat distorted structure exhibited by the films as compared to the two-line ferrihydrite synthesized. The signals from the Fe···C distances and those reflecting Fe–O–C three leg, back-scattering (signals from materials other than Fe(III) (hydr)oxide minerals) were detected in films from two other sampling

locations and the proportion of the Fe(III) bound to natural organic matter was estimated to be 60–70%. The film samples from these two other sampling sites showed shorter Fe···Fe distances that reflect the distance known for the geometrics of the octahedral edge-sharing Fe(III) present in ferrihydrite [37].

We consider that the following possibility might not be ruled out with respect to the observations and interpretations above: The differences in the EXAFS signals for the films from different sampling sources/locations could also partially be due to the differences in age of the film samples at time of sampling, since the films actually could resume different polymeric or mineralogical structures along the sequential stages of their formation and transformation. In other words, the floating Fe(III) films may vary not only from location to location (spatial factor), but also from time to time (temporal factor) in the same location along their formation and transformation/aging.

Characteristics of Ferrihydrite: Ferrihydrite is known as one of the soil Fe(III) oxide and oxyhydroxide minerals that has received sizable attention [20,21,87]. It was named by Chukhrov et al. [88] and accepted as a mineral in 1971 by the Nomenclature Commission of the International Mineralogical Association. It was previously called “amorphous ferric hydroxide” because it is a poorly ordered Fe(III) oxide species. This mineral can be found in some particular soil-associated environments such as drainage ditches and small, slow running water courses and in places where Fe(II) is oxidized and then precipitates in the presence of rich organic substances [20,21,87].

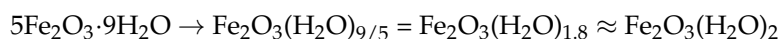
Ferrihydrite is generated by Fe(III) hydrolysis. It is a widespread and characteristic component of young Fe-oxide accumulations from ferriferous water. Ferrihydrite appears as rusty voluminous precipitates rich with adsorbed water, inorganic ions, some silicates and phosphates, and organic substances. It is commonly present as very small colloidal spherical particles (3–7 nm in diameter), highly aggregated. Ferrihydrite has short-range ordering that exhibits broad X-ray diffraction lines and thus it is not a true hydroxide. Ferrihydrite has a distinct analytical feature, i.e., it is considerably or nearly completely soluble in acid ammonium oxalate in the dark [20,21,87].

Ferrihydrite bears the following physical characteristics: a density of 3.96 g cm⁻³, very small particle sizes (50–100 Å), high surface areas (200–350 or 100–700 m² g⁻¹, 2–5 × 10⁵ m² kg⁻¹), reddish-brown colors (generally, 2.5YR–5YR–7.5YR in the *Munsell Soil Color Charts*, e.g., 2.5YR3/6, more reddish than goethite, less reddish than hematite), a trigonal crystal system, and a spherical crystal morphology. It is structurally quite close to hematite, but it has some structural defects, e.g., replacement of some O (and OH) by water molecules and some vacant Fe positions [20,21,87].

Ferrihydrite can be easily synthesized by microbial oxidation of Fe(II) citrate solution or some natural carbon-rich samples. Further crystallization is retarded by adsorption of environmental impurities, especially some organic substances, on very small amorphous colloids of high surface areas. Ferrihydrite can form rather fast, but this mineral actually does not stay as a stable mineral phase. Eventually, it transforms to become a more stable crystalline form of goethite (α-FeOOH) in humid temperate regions, or hematite (α-Fe₂O₃) in warm and dry environments [20,21,87]. The physical and chemical characteristics of ferrihydrite and the ambient environments for its formation appear to be quite consistent with the findings about the observed floating Fe(III) films as reported in various published studies as well as the present investigation [20,21,37–40,87].

Composition formula for Ferrihydrite: The bulk composition (not structure) formula for ferrihydrite is considered to be 5Fe₂O₃·9H₂O [21,87]. This indicates that it is rich in water and may account for its voluminous nature as very small colloidal particles [21,87].

The composition of 5Fe₂O₃·9H₂O for ferrihydrite can be viewed in another form:

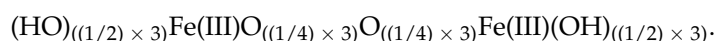


Considering that, respectively, Fe(OH)₃ and FeOOH can be viewed as Fe₂O₃(H₂O)₃ and Fe₂O₃(H₂O)₁, it is interesting to notice that Fe₂O₃(H₂O)₂ for ferrihydrite stands just in between Fe(OH)₃ (i.e., Fe₂O₃(H₂O)₃) and FeOOH (i.e., Fe₂O₃(H₂O)₁). This seems to

suggest that ferrihydrite is probably composed of a mixture of various Fe(III) polymers in the form of $\text{Fe}_2\text{O}_3(\text{H}_2\text{O})_{n=1-3}$, rather than a single mineral with a well-defined composition. It may also exist as an intermediate polymer species between $\text{Fe}(\text{OH})_3$ and FeOOH .

An elaboration provides support for the above notion regarding the interpretation of $\text{Fe}_2\text{O}_3(\text{H}_2\text{O})_{1.8}$ as the composition of ferrihydrite. To facilitate the illustration, a new Fe(III) polymer species is enlisted here. This polymer has two layers of Fe(III) and a composition in between the $\text{Fe}(\text{OH})_3$ polymer with one Fe(III) layer (see Figure 9a) and the FeOOH polymer with three Fe(III) layers (see Figure 9b).

This new polymer sheet can form by fusing a one-Fe(III)-layer $\text{Fe}(\text{OH})_3$ polymer sheet with another identical $\text{Fe}(\text{OH})_3$ sheet, with a segment of the $\text{Fe}(\text{OH})_3$ sheet, or simply with a single piece or individual pieces of $\text{Fe}(\text{OH})_3$ monomers or dimers, etc. This polymer has five layers, $\text{HO-Fe(III)-O-Fe(III)-OH}$, and the two Fe(III) layers are identical. These have three inner O ions, each sharing with four Fe(III) ions, and three outer O ions, each sharing with two Fe(III) ions as OH groups in the Fe(III)O_6 unit (Table 12). The middle O ions sharing with four Fe(III) ions fuse the two Fe(III) layers together:



The composition formula can be found for this new Fe(III) polymer as follows: For the O sharing with four Fe(III) ions in the middle, each O contributes $(1/4)\text{O}$ to the Fe(III), while for the O sharing with two Fe(III) in the OH groups on the sides (top, bottom), each O gives $(1/2)\text{OH}$ to the Fe(III). Hence, each of the two identical Fe(III) ions considered from the two Fe(III) layers gets $(1/4)\text{O} \times 3 + (1/2)\text{OH} \times 3$ for one Fe(III)O_6 unit. Thus, two of the Fe(III) ions in total have $((1/4)\text{O} \times 3 + (1/2)\text{OH} \times 3) \times 2 = (3/2)\text{O} + 3(\text{OH})$. This results in the following composition formula: $2\text{Fe}(3/2)\text{O}3(\text{OH}) = 2\text{Fe}3\text{O}(3/2)\text{O}3\text{H} = \text{Fe}_2\text{O}_3(\text{H}_2\text{O})_{(3/2)} = \text{Fe}_2\text{O}_3(\text{H}_2\text{O})_{1.5}$.

A charge balance can be determined for this new polymer. Each O sharing with four Fe(III) ions gives $(-2)/4 = -1/2$ charge to the central Fe(III), while each side O sharing with two Fe(III) ions contributes $(-1)/2$ charge to the central Fe(III) (remaining -1 balanced by H^+ as OH group). Hence, the total charge from six O ions around the central Fe(III) amounts to $(-1/2) \times 3 + (-1/2) \times 3 = -3$, balancing $+3$ of the central Fe(III) (Table 12).

With the new Fe(III) polymer species of two Fe(III) layers ($\text{Fe}_2\text{O}_3(\text{H}_2\text{O})_{1.5}$) introduced, ferrihydrite ($\text{Fe}_2\text{O}_3(\text{H}_2\text{O})_{1.8}$) actually falls in between $\text{Fe}_2\text{O}_3(\text{H}_2\text{O})_3$ ($\text{Fe}(\text{OH})_3$ polymer of one Fe(III) layer) and $\text{Fe}_2\text{O}_3(\text{H}_2\text{O})_{1.5}$ (the new Fe(III) polymer of two Fe(III) layers). In other words, ferrihydrite is probably composed of various Fe(III) polymer species in the form of $\text{Fe}_2\text{O}_3(\text{H}_2\text{O})_{n=1.5-3}$, instead of $\text{Fe}_2\text{O}_3(\text{H}_2\text{O})_{n=1-3}$, as tentatively considered previously.

Furthermore, the irregular number of 1.8 for water in the ratios of the composition of ferrihydrite seems to suggest that it could be a mixture of $\text{Fe}_2\text{O}_3(\text{H}_2\text{O})_3$ and $\text{Fe}_2\text{O}_3(\text{H}_2\text{O})_{1.5}$ at certain proportions. One scenario of such a kind can be revealed as follows: We assume that ferrihydrite has a composition of $3x + 1.5y = 1.8$ (where $x + y = 1$, and x and y are the proportions (%) of $\text{Fe}_2\text{O}_3(\text{H}_2\text{O})_3$ and $\text{Fe}_2\text{O}_3(\text{H}_2\text{O})_{1.5}$, respectively) to yield the overall $\text{Fe}_2\text{O}_3(\text{H}_2\text{O})_{1.8}$ for ferrihydrite. The equation $3x + 1.5y = 1.8$ can be transformed to $3x + 1.5 \times (1 - x) = 1.8$ since $x + y = 1$. Solving x yields $x = 0.2$ (20%). This can be verified by the following calculation: $3 \times 0.2 + 1.5 \times 0.8 = 1.8$. This calculation shows that with respect to the scenario considered here, ferrihydrite can be composed of a mixture of 20% $\text{Fe}_2\text{O}_3(\text{H}_2\text{O})_3$ and 80% $\text{Fe}_2\text{O}_3(\text{H}_2\text{O})_{1.5}$ with both polymers of well-defined composition and structure in separate pure particles.

Alternatively, ferrihydrite in the above proportions of 20% and 80% can materialize in another way. This polymer can be viewed as an incomplete $\text{Fe}_2\text{O}_3(\text{H}_2\text{O})_{1.5}$ polymer (two Fe(III) layers) in one single piece with 20% of its polymer body only having one Fe(III) layer (defect) as the $\text{Fe}_2\text{O}_3(\text{H}_2\text{O})_3$ polymer ($\text{Fe}(\text{OH})_3$ polymer). In other words, ferrihydrite can also be viewed as an $\text{Fe}_2\text{O}_3(\text{H}_2\text{O})_3$ polymer in one piece with 80% of its body covered (or fused) with another layer or groups of Fe(III) to become the $\text{Fe}_2\text{O}_3(\text{H}_2\text{O})_{1.5}$ polymer. The spots of the one-Fe(III)-layer polymer (the original $\text{Fe}(\text{OH})_3$ sheet) may be concentrated in certain locations or sections of the original $\text{Fe}(\text{OH})_3$ polymer or randomly spread at single

spots or groups of spots. The distribution depends on the conditions and availability of the $\text{Fe}(\text{OH})_3$ monomers and dimers and segments of the $\text{Fe}(\text{OH})_3$ polymers as precursors. The discussion on ferrihydrite thus reinforces the notion that it is probably composed of various Fe(III) polymers, complete and incomplete in terms of well-defined structures.

A number of other formulae were also proposed for the composition of ferrihydrite, including $\text{Fe}_5\text{HO}_8 \cdot 4\text{H}_2\text{O}$ ($=\text{Fe}_5\text{O}_{7.5}\text{HO}_{0.5}4\text{H}_2\text{O} = (\text{Fe}_2\text{O}_3)_{2.5}(\text{H}_2\text{O})_{0.5}4\text{H}_2\text{O} = (\text{Fe}_2\text{O}_3)_{2.5}(\text{H}_2\text{O})_{4.5} = \text{Fe}_2\text{O}_3(\text{H}_2\text{O})_{(4.5/2.5)} = \text{Fe}_2\text{O}_3(\text{H}_2\text{O})_{1.8} \rightarrow 5\text{Fe}_2\text{O}_3 \cdot 9\text{H}_2\text{O}$); $\text{Fe}_5(\text{O}_4\text{H}_3)_3$ ($=\text{Fe}_5\text{O}_{12}\text{H}_9 = \text{Fe}_5\text{O}_{7.5}\text{O}_{4.5}\text{H}_9 = (\text{Fe}_2\text{O}_3)_{2.5}(\text{H}_2\text{O})_{4.5} = \text{Fe}_2\text{O}_3(\text{H}_2\text{O})_{1.8} \rightarrow 5\text{Fe}_2\text{O}_3 \cdot 9\text{H}_2\text{O}$); and $\text{Fe}_2\text{O}_3 \cdot 2\text{FeOOH} \cdot 2.6\text{H}_2\text{O}$ ($=\text{Fe}_2\text{O}_3\text{Fe}_2\text{O}_2\text{O}_2\text{H}_2(\text{H}_2\text{O})_{2.6} = \text{Fe}_2\text{O}_3\text{Fe}_2\text{O}_3\text{OH}_2(\text{H}_2\text{O})_{2.6} = (\text{Fe}_2\text{O}_3)_2(\text{H}_2\text{O})_{3.6} = \text{Fe}_2\text{O}_3(\text{H}_2\text{O})_{1.8} \rightarrow 5\text{Fe}_2\text{O}_3 \cdot 9\text{H}_2\text{O}$) [20,21,87]. Interestingly, all these other forms of ferrihydrite actually share the same (equivalent) composition of $5\text{Fe}_2\text{O}_3 \cdot 9\text{H}_2\text{O}$.

3.8. General Composition Formula for Various Fe(III) Polymers

Our discussion has shown that floating Fe(III) films are composed of various Fe(III) polymers (e.g., $\text{Fe}(\text{OH})_3$, FeOOH , or Fe_2O_3) and ferrihydrite is composed of various Fe(III) polymers ($\text{Fe}_2\text{O}_3(\text{H}_2\text{O})_{n=1.5-3}$). Clearly, the various Fe(III) polymers are at the center of the Fe(III) films with respect to their composition and structure. Our previous discussions on $\text{Fe}(\text{OH})_3$ ($\text{Fe}_2\text{O}_3(\text{H}_2\text{O})_3$), $\text{Fe}_2\text{O}_3(\text{H}_2\text{O})_{1.5}$, FeOOH ($\text{Fe}_2\text{O}_3(\text{H}_2\text{O})_1$), and Fe_2O_3 ($\text{Fe}_2\text{O}_3(\text{H}_2\text{O})_0$) all converge to a certain regularity shared by these various Fe(III) polymers concerning their composition and structure. This regularity leads to an emergence of a general composition formula corresponding to the general structure for the Fe(III) polymers of multiple Fe(III) layers ($m = 1, 2, 3, \dots$, where m is the number of Fe(III) layers in the Fe(III) polymers).

The introduction of a new Fe(III) polymer of four Fe(III) layers should be helpful to the derivation of the general composition formula. As shown in the case of FeOOH ($\text{Fe}_2\text{O}_3(\text{H}_2\text{O})_1$, $m = 3$), this new polymer shares the same structure feature corresponding to its composition: two identical middle Fe(III) layers in between two identical outside Fe(III) layers (top and bottom). This feature can serve as a general structure model for various Fe(III) polymers of multiple layers of Fe(III), no matter how many middle Fe(III) layers.

Like FeOOH (Figure 9b, Table 12), this new polymer has the following composition corresponding to its structure with four Fe(III) ions considered for the four Fe(III) layers ($m = 4$, two outside, two middle):

$$\begin{aligned} & \{\text{Fe(III)(OH)}_{((1/2) \times 3)}\text{O}_{((1/4) \times 3)}\}\{\text{Fe(III)O}_{((1/4) \times 6)}\}\{\text{Fe(III)O}_{((1/4) \times 6)}\}\{\text{Fe(III)O}_{((1/4) \times 3)}(\text{OH})_{((1/2) \times 3)}\} \\ & \text{Fe(III)}_4\text{O}_{((1/4) \times 3 + (1/4) \times 6 + (1/4) \times 6 + (1/4) \times 3)}(\text{OH})_{((1/2) \times 3 + (1/2) \times 3)} \\ & \text{Fe(III)}_4\text{O}_{((1/4) \times 6 \times 2 + (1/4) \times 3 \times 2)}(\text{OH})_{((1/2) \times 3 \times 2)} = \text{Fe(III)}_4\text{O}_{((1/4) \times 6 \times (4-1))}(\text{OH})_3 \quad (m = 4) \\ & = \text{Fe(III)}_4\text{O}_{(3+3/2)}(\text{OH})_3 = \text{Fe}_2\text{O}_3\text{Fe}_2\text{O}_3\text{O}_{3/2}\text{H}_3 = (\text{Fe}_2\text{O}_3)_2(\text{H}_2\text{O})_{3/2} \rightarrow \text{Fe}_2\text{O}_3(\text{H}_2\text{O})_{3/4}. \end{aligned}$$

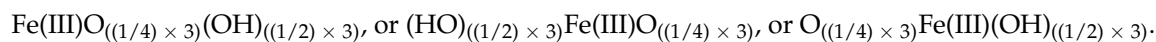
A comparison of the derivation for the FeOOH polymer of three Fe(III) layers ($m = 3$, composition formula: $\text{Fe(III)}_3\text{O}_{((1/4) \times 6 \times (3-1))}(\text{OH})_3$) with that for the new Fe(III) polymer of four Fe(III) layers ($m = 4$, composition formula: $\text{Fe(III)}_4\text{O}_{((1/4) \times 6 \times (4-1))}(\text{OH})_3$) can inductively yield the general composition formula for various Fe(III) polymers of multiple layers of Fe(III) ($m = 1, 2, 3, 4, \dots$) in an identical manner, as shown below.

Considering a general structure model for all various Fe(III) polymers of multiple layers of Fe(III), they all share the same structure feature: $(m - 2)$ identical middle layers of the same Fe(III) wrapped in between two identical outside layers (top and bottom) of Fe(III) (the sandwich structure). Hence, the following general formula for the various multi-Fe(III)-layer polymers can readily be inferred inductively, by replacing, e.g., 4, with m in the composition formula of $\text{Fe(III)}_4\text{O}_{((1/4) \times 6 \times (4-1))}(\text{OH})_3$ for $\text{Fe}_2\text{O}_3(\text{H}_2\text{O})_{3/4}$ ($m = 4$):

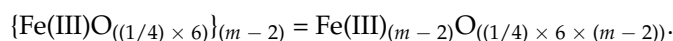
$$\text{Fe(III)}_m\text{O}_{((1/4) \times 6 \times (m-1))}(\text{OH})_3 \quad m = \text{total number of Fe(III) layers.}$$

A formal derivation of the general composition formula can be formulated as follows: Corresponding to the general structure of the Fe(III) polymers of multiple (m) layers of Fe(III) as described above, we can consider one Fe(III) for one Fe(III) layer, and so here

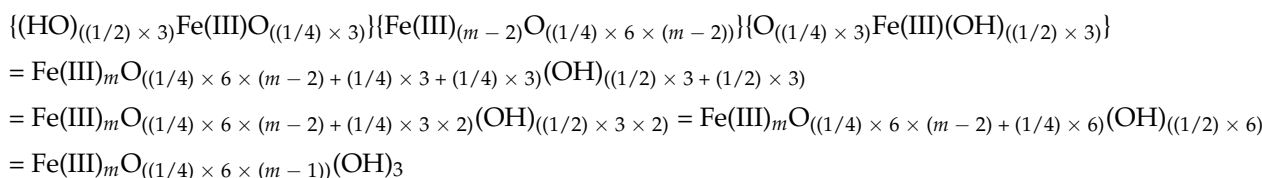
we have m Fe(III) ions considered in total (two outside layer Fe(III) ions (top and bottom) and $(m - 2)$ middle layer Fe(III) ions). Each of the two identical outside layer Fe(III) ions considered has three inner O ions, each shared with four central Fe(III) ions, and three outer OH groups, each shared with two central Fe(III) ions in its octahedral Fe(III)O₆ unit. As a result, the outside layer Fe(III) each has the following composition:



On the other hand, each of the identical middle-layer Fe(III) ions considered has six O ions in its Fe(III)O₆ unit, each shared with four central Fe(III) ions, and its composition thus is Fe(III)O_{((1/4) × 6)}. For a total of $(m - 2)$ identical middle-layer Fe(III) ions considered, their overall composition is as follows:

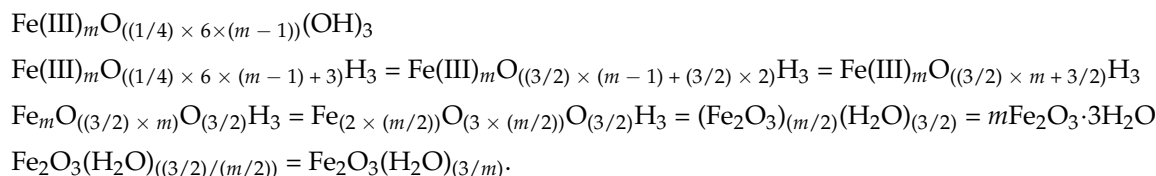


It follows that the entire polymer holds the following composition corresponding to its structure of $(m - 2)$ middle layers of Fe(III) in between two outside layers of Fe(III):



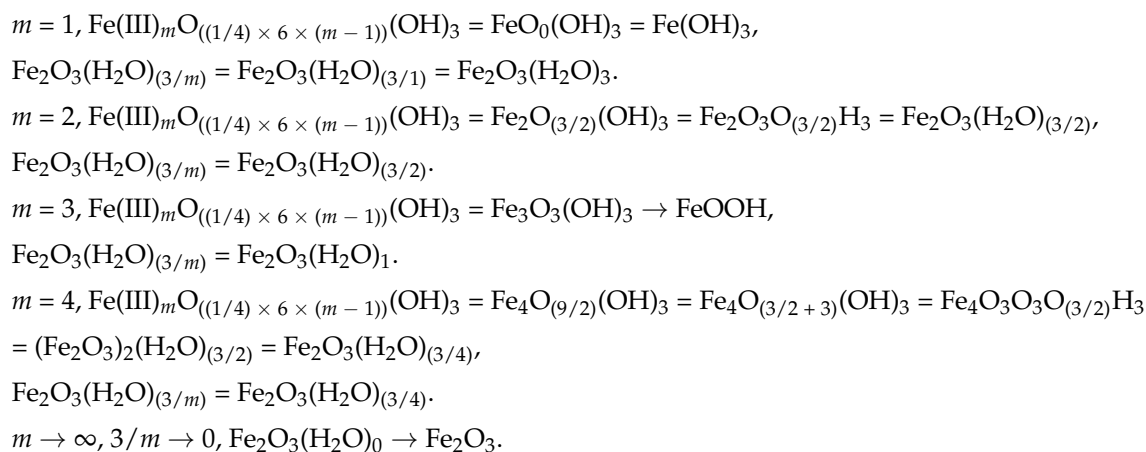
The above composition formula exactly resembles the one obtained intuitively as just shown by comparing the two formulae for the two Fe(III) polymers ($m = 3, m = 4$).

The general formula corresponding to the above composition formula in terms of Fe₂O₃ and H₂O as hydrous ferric oxides ($m\text{Fe}_2\text{O}_3 \cdot n\text{H}_2\text{O}$) can be derived as follows:



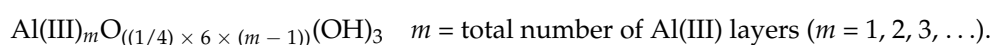
The above formula is a manifestation of the condensation polymerization through water elimination during formation and transformation of various Fe(III) polymers ($m = 1, 2, 3, 4, \dots$).

The above derivations for the general formulae can be verified by assigning the m numbers to yield the specific corresponding formulae:



The above specification for the verification generates the identical outcomes of the compositions of the Fe(III) polymers presented previously. This thus leads to the general notion that Fe(III) films are composed of various Fe(III) polymers of multiple layers of Fe(III) that hold a general, unified composition formula, i.e., $\text{Fe}_m\text{O}_{((1/4) \times 6 \times (m-1))}(\text{OH})_3$ or $\text{Fe}_2\text{O}_3(\text{H}_2\text{O})_{(3/m)}$ ($m = 1, 2, 3, 4, \dots$), as complete (defined by the composition formula) and/or incomplete (partially formed, with defects) forms of the Fe(III) polymers.

The formulation and discussion on the formation and transformation of the various Fe(III) polymers can be applicable to the case of Al(III) as well. Like Fe(III), Al(III) is a typical Brønsted–Lowry acid (an ion or a molecule that can release/donate proton(s) in an aqueous solution or water). Al(III) ions hydrolyze in water, and various products of Al(III) hydrolysis polymerize to become stable. The polymerization of various Al(III) hydrolysis products and transformation of various Al(III) polymers thus resemble those for the Fe(III) species. Hence, the general composition formula for various Al(III) polymers can readily be obtained by replacing Fe(III) with Al(III) in the formula for Fe(III), as given below:



Likewise, it follows that the composition formula in terms of Al_2O_3 and H_2O as hydrous aluminum oxides ($m\text{Al}_2\text{O}_3 \cdot n\text{H}_2\text{O}$) also holds true for the Al(III) polymers: $\text{Al}_2\text{O}_3(\text{H}_2\text{O})_{(3/m)}$.

3.9. Significance and Applications

The significance and potential applications relevant to our study can be recognized as follows:

Method for generation of floating Fe(III) films in a laboratory setting: A method was developed that can deliver the Fe(III) films in a controllable laboratory setting. This setup only requires fresh soils (Fe(III) and microbe sources), glucose (energy source), and water. This method can offer multiple renewable harvests of the Fe(III) films by repeatedly using the same setup with the same soil upon fresh addition of sugar. This setup can be scaled up to manufacture films with large sizes and quantities by domesticizing the soil microbes via laboratory farming. With this method, Fe(III) films of rich varieties in thickness, size, morphology, and structure across various stages of formation and transformation become available. A variety of films can be obtained as desired, from very thin, colorless, initial films with reflective rainbow iridescence; to colored thickened films; and, eventually, to orange/orange-red/red crusts.

Platform for further investigation into the floating Fe(III) film phenomenon: This method offers an assessable, controllable laboratory platform for further studies on the kinetics, mechanism, and process of biotic and abiotic (chemical) nature and controlling factors (e.g., organic acids and ligands) involved in the floating Fe(III) film phenomenon.

Environmental formation and transformation of Fe(III) hydroxides, oxyhydroxides, and oxides: Formation and transformation of hydroxides, oxyhydroxides, and oxides of Fe(III) can be difficult to separate from their in situ soil or sediment environments. It is challenging to obtain a platform that can offer the formation and transformation of these Fe(III) species separated from their environments. Our Fe(III) film generation method thus provides a useful means to observe and obtain a variety of Fe(III) films (i.e., various Fe(III) species) so as to conduct compositional and structural analyses to study their formation and transformation separately. This platform is advantageous in providing the films (Fe(III) species) generated at various stages (especially the initial stages, which are hard to catch in situ).

Potential versatile roles of Fe(III) nanofilms: With various Fe(III) films available as desired, new research may become accessible or accomplishable to further explore the versatile roles of the Fe(III) films as nanofilms in Fe(III)/Fe(II)/surface-catalyzed chemical and photochemical reactions involving transformations of various natural and synthetic chemical compounds. It is thus perceivable that the nanofilm-catalyzed reactions might extend to environmentally significant transformations, such as decomposition of water to generate hydrogen (H_2), artificial photosynthesis, and chemical conversion of CO_2 to

methanol and other organic compounds of various uses, which may lead to novel avenues to provide new, green energy sources and materials and replace plastic materials made of petroleum products. The potential of nanofilms in various applications surely warrants further innovative exploration.

4. Conclusions

The following conclusions can be drawn from the present research:

- (1) A method was successfully developed, capable of delivering floating Fe(III) films in an assessable, controllable laboratory setting. This method can provide a renewable supply of floating Fe(III) films as desired. Furthermore, this setup can be scaled up to manufacture Fe(III) films with large sizes and quantities. With this method now available, Fe(III) films of rich varieties in thickness, size, morphology, and structure across all stages of the formation and transformation can be made available. A variety of the Fe(III) films can be collected for various compositional and structural analyses. Moreover, this laboratory setup offers a controlled experimental platform for further investigation into the kinetics, mechanism, process, and controlling factors involved in the floating Fe(III) film phenomenon.
- (2) With a variety of the Fe(III) films now available, new, creative research may become potentially accessible or accomplishable to explore the versatile roles of the Fe(III) films as nanofilms in various Fe(III)/Fe(II)/surface-catalyzed chemical and photochemical reactions that involve transformations of a variety of natural and synthetic compounds for various applications.
- (3) A comprehensive mechanistic picture of the formation of floating Fe(III) films with technical details was formulated in connection with the results of our experimental work. The floating Fe(III) film phenomenon is an environmental chemical drama of the redox cycling of Fe(III)/Fe(II) species at soil/water and water/air interfaces (redox interfaces or boundaries controlled by oxygen gradient) coupled with Fe(II) transport from soil particles to the water surface, as shown by a summative depiction (Figure 11), followed by ultimate mineralization of the Fe(III) polymers of the Fe(III) films.
- (4) A polymeric model was created to account for the transformation of the Fe(III) films over their entire span. According to this model, various products of the hydrolysis of Fe(III) from oxidation of microbially generated Fe(II) spontaneously polymerize to stabilize by forming a complex variety of Fe(III) polymers, from Fe(III) dimers and trimers, to elongated linear Fe(III) polymers, to 2D Fe(III) polymer sheets, to 3D Fe(III) polymer assemblies, and eventually to Fe₂O₃ colloids. Floating Fe(III) films are essentially composed of a rich repertoire of various intermediate and incomplete as well as completely formed (well-defined) Fe(III) polymers with multiple layers (*m* layers) of Fe(III), as a complex mixture. These Fe(III) polymers form by condensation polymerization via elimination of water molecules through edge-sharing of the Fe(III)O₆ octahedral units (i.e., O sharing between Fe(III) ions). The various Fe(III) polymers of defined compositions hold a general, unified composition formula, Fe_{*m*}O_{((1/4) × 6 × (*m* - 1))}(OH)₃ or Fe₂O₃(H₂O)_(3/*m*) (*m* = 1, 2, 3, 4, ...).

The environmental chemistry of iron is fascinating. The natural wonder of the Fe(III) films floating on water surfaces in the environment certainly invites the attention of curious minds.

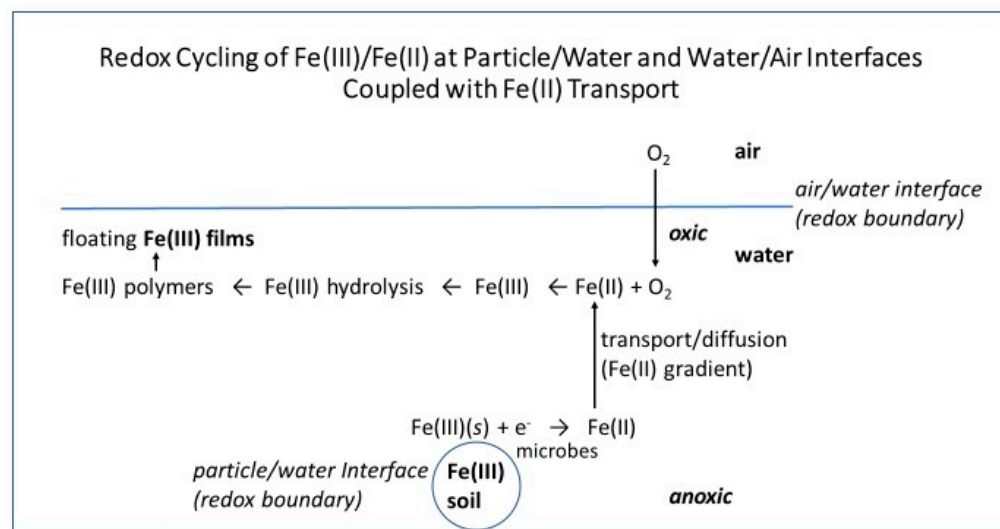


Figure 11. A schematic picture of the redox cycling of Fe(III)/Fe(II) at particle/water and water/air interfaces coupled with Fe(II) transport involved in the floating Fe(III) film phenomenon.

Author Contributions: Conceptualization, H.Z.; Investigation, Z.R., Z.P., K.D., S.A., C.C., Z.C., S.C., C.M. and H.Z.; Methodology, H.Z.; Project administration, H.Z.; Resources, H.Z.; Supervision, H.Z.; Writing—original draft, H.Z.; Writing—editing, H.Z. All authors have read and agreed to the published version of the manuscript.

Funding: This research received no external funding.

Data Availability Statement: Data is contained within the article.

Acknowledgments: This paper is dedicated to Rich Bartlett. Jonathan Dupuy, Danner Keeton, and Luck Overton participated in some of the research mentioned in the present paper.

Conflicts of Interest: The authors declare no conflicts of interest.

References

- Norman, E.B. Stellar alchemy: The origin of the chemical elements. *J. Chem. Ed.* **1994**, *71*, 813–820. [[CrossRef](#)]
- Selbin, J. The origin of the chemical elements 1. *J. Chem. Ed.* **1973**, *50*, 306–310. [[CrossRef](#)]
- Selbin, J. The origin of the chemical elements 2. *J. Chem. Ed.* **1973**, *50*, 380–387. [[CrossRef](#)]
- Viola, V.E. Formation of the chemical elements and the evolution of our universe. *J. Chem. Ed.* **1990**, *67*, 723–730. [[CrossRef](#)]
- Henderson, P. *Inorganic Geochemistry*; Pergamon Press: New York, NY, USA, 1982.
- Mason, B. *Principles of Geochemistry*; John Wiley & Sons: New York, NY, USA, 1966.
- Cox, P.A. *The Elements on Earth*; Oxford University Press: Oxford, UK, 1995.
- Stefansson, A. Iron(III) hydrolysis and solubility at 25 °C. *Environ. Sci. Technol.* **2007**, *41*, 6117–6123. [[CrossRef](#)]
- Skinner, B.J.; Porter, S.C. *Dynamic Earth an Introduction to Physical Geology*, 4th ed.; John Wiley & Sons: New York, NY, USA, 2000.
- Jjemba, P.K. *Environmental Microbiology, Principles and Applications*; Science Publishers, Inc.: Enfield, NH, USA, 2004.
- Schneider, W.; Schwyn, B. The hydrolysis of iron in synthetic, biological, and aquatic media. In *Aquatic Surface Chemistry: Chemical Processes at the Particle-Water Interface*; Stumm, W., Ed.; Wiley-Interscience: New York, NY, USA, 1987.
- da Silva, J.J.R.F.; Williams, R.J.P. *The Biological Chemistry of the Elements: The Inorganic Chemistry of Life*; Oxford University Press: Oxford, UK, 1991.
- Silver, S. Genes for all metals—A bacterial view of the periodic table the 1996 Thom Award Lecture. *J. Indust. Microbio. Biotech.* **1998**, *20*, 1–12. [[CrossRef](#)] [[PubMed](#)]
- Williams, R.J.P.; da Silva, J.J.R.F. *The Natural Selection of the Chemical Elements, the Environment and Life's Chemistry*; Oxford University Press: Oxford, UK, 1996.
- Lehninger, A.L.; Nelson, D.L.; Cox, M.M. *Principles of Biochemistry*, 2nd ed.; Worth Publishers: New York, NY, USA, 1993.
- Nicholls, D. *Comprehensive Inorganic Chemistry*; Bailar, J.C., Emeleus, H.J., Nyholm, R., Trotman-Dickerson, A.F., Eds.; Pergamon Press: Elmsford, NY, USA, 1973; Volume III.
- Bailey, R.A.; Clark, H.M.; Ferris, J.P.; Krause, S.; Strong, R.L. *Chemistry of the Environment*, 2nd ed.; Academic Press: San Diego, CA, USA, 2002.
- Bartlett, R.J. Soil redox behavior. In *Soil Physical Chemistry*; Sparks, D.L., Ed.; CRC Press: Boca Raton, FL, USA, 1986.

19. Bartlett, R.J.; James, B.R. Redox chemistry of soils. *Adv. Agron.* **1993**, *50*, 151–208.
20. Essington, M.E. *Soil and Water Chemistry an Integrative Approach*; CRC Press: Boca Raton, FL, USA, 2004.
21. Schwertmann, U.; Taylor, R.M. Iron oxides. In *Minerals in Soil Environments*, 1st ed.; Dixon, J.B., Weed, S.B., Eds.; Soil Science Society of America: Madison, WI, USA, 1977.
22. Rizzolo, J.A.; Barbosa, C.G.G.; Borillo, G.C.; Godoi, A.F.L.; Souza, R.A.F.; Andreoli, R.V.; Manzi, A.O.; Sá, M.O.; Alves, E.G.; Pöhlker, C.; et al. Soluble iron nutrients in Saharan dust over the central Amazon rainforest. *Atmos. Chem. Phys.* **2017**, *17*, 2673–2687. [[CrossRef](#)]
23. Martin, J.H. Iron as a limiting factor in oceanic productivity. In *Primary Productivity and Biogeochemical Cycles in the Sea*; Falkowski, P.G., Woodhead, A.D., Vivirito, K., Eds.; Environmental Science Research; Springer: Boston, MA, USA, 1992; Volume 43. [[CrossRef](#)]
24. Martin, J.H.; Coale, K.H.; Johnson, K.S.; Fitzwater, S.E.; Gordon, R.M.; Tanner, S.J.; Hunter, C.N.; Elrod, V.A.; Nowicki, J.L.; Coley, T.L.; et al. Testing the iron hypothesis in ecosystems of the equatorial Pacific Ocean. *Nature* **1994**, *371*, 123–129. [[CrossRef](#)]
25. Rose, A.L.; Waite, T.D. kinetics of hydrolysis and precipitation of ferric iron in seawater. *Environ. Sci. Technol.* **2003**, *37*, 3897–3903. [[CrossRef](#)]
26. Stumm, W.; Morgan, J.J. *Aquatic Chemistry*, 3rd ed.; John Wiley & Sons: New York, NY, USA, 1996; pp. 478–479.
27. Barbeau, K.; Rue, E.L.; Bruland, K.W.; Butler, A. Photochemical cycling of iron in the surface ocean mediated by microbial iron(III)-binding ligands. *Nature* **2001**, *413*, 409–413. [[CrossRef](#)]
28. Brezonik, P.L. *Chemical Kinetics and Process Dynamics in Aquatic Systems*; Lewis Publishers: Boca Raton, LA, USA, 1994; pp. 257–267.
29. Zhang, H.; Bartlett, R. Light-induced oxidation of aqueous chromium(III) in the presence of iron(III). *Environ. Sci. Technol.* **1999**, *33*, 588–594. [[CrossRef](#)]
30. Zhang, H.; Lindberg, S. Sunlight and Fe(III)-induced photochemical production of dissolved gaseous mercury in freshwater. *Environ. Sci. Technol.* **2001**, *35*, 928–935. [[CrossRef](#)] [[PubMed](#)]
31. Zuo, Y.; Hoigne, J. Formation of hydrogen peroxide and depletion of oxalic acid in atmospheric water by photolysis of iron(III)-oxalato complexes. *Environ. Sci. Technol.* **1992**, *26*, 1014–1022. [[CrossRef](#)]
32. Jacobson, M.C.; Charlson, R.J.; Rodhe, H.; Orians, G.H. *Earth System Science from Biogeochemical Cycles to Global Change*; Academic Press: San Diego, CA, USA, 2000.
33. Morel, F.M.M.; Hering, J.G. *Principles and Applications of Aquatic Chemistry*; John Wiley & Sons: New York, NY, USA, 1993; pp. 482–494.
34. Davison, W. Conceptual models for transport in a redox boundary. In *Chemical Processes in Lakes*; Stumm, W., Ed.; Wiley-Interscience: New York, NY, USA, 1985.
35. Alexander, M. *Introduction to Soil Microbiology*; John Wiley & Sons: New York, NY, USA, 1977.
36. Zajic, J.E. *Microbial Biochemistry*; Academic Press: New York, NY, USA, 1969.
37. Kleja, D.B.; van Schaik, J.W.J.; Persson, I.; Gustafsson, J.P. Characterization of iron in floating surface films of some natural waters using EXAFS. *Chem. Geol.* **2012**, *326–327*, 19–26. [[CrossRef](#)]
38. Grathoff, G.; Baham, J.; Easterly, H.; Gassman, P.; Hugo, R. Mixed-valent Fe films (schwimmeisen) on the surface of reduced ephemeral pools. *Clays Clay Miner.* **2007**, *55*, 638–646. [[CrossRef](#)]
39. Perkins, R.B.; Gray, Z.N.; Grathoff, G.; Hugo, R. Characterization of natural and synthetic floating iron surface films and their associated waters. *Chem. Geol.* **2016**, *444*, 16–26. [[CrossRef](#)]
40. Reina, M.; Portillo, M.C.; Serrano, L.; Lucassen, E.C.H.E.T.; Roelofs, J.G.M.; Romero, A.; Gonzalez, J.M. The interplay of hydrological, chemical and microbial processes in the formation of iron-rich floating films in aquatic environments at a circumneutral pH. *Limnologia* **2015**, *34*, 365–380.
41. Dunn, K.; Asmus, K.; Cooke, C.; Cord, Z.; Coulter, S.; Morris, C.; Zhang, H. Abiotic generation of floating iron (Fe) hydroxide film with rainbow reflection: A preliminary hypothesis testing study. In Proceedings of the 17th Annual Research & Creative Inquiry Day, Cookeville, TN, USA, 21 April 2022; Proceedings 2022.indd (tntech.edu). Tennessee Tech University: Cookeville, TN, USA, 2022; p. 3.
42. Rush, Z.; Penn, Z.; Zhang, H. Microbially mediated generation of floating iron (Fe) (oxy)hydroxide-oxide film in inundated soils: A preliminary laboratory study. In Proceedings of the 17th Annual Research & Creative Inquiry Day, Cookeville, TN, USA, 21 April 2022; Proceedings 2022.indd (tntech.edu). Tennessee Tech University: Cookeville, TN, USA, 2022; p. 41.
43. Langmuir, D.L. *Aquatic Environmental Geochemistry*; Prentice Hall: Upper Saddle River, NJ, USA, 1997; pp. 420–421.
44. Leenheer, J.A.; Malcolm, R.L.; McKinley, P.W.; Eccles, L.A. Occurrence of dissolved organic carbon in selected groundwater samples of the United States. *US Geol. Surv. J. Res.* **1974**, *2*, 361–369.
45. Berner, R.A. A new geochemical classification of sedimentary environments. *J. Sediment. Res.* **1981**, *51*, 359–365.
46. Levett, P.N. *Anaerobic Bacteria a Functional Biology*; Open University Press: Philadelphia, MA, USA, 1990.
47. Ghiorse, W.C. Microbial reduction of manganese and iron. In *Biology of Anaerobic Microorganisms*; Zehnder, A.J., Ed.; Wiley-Interscience: New York, NY, USA, 1988.
48. Kirchman, D.L. *Processes in Microbial Ecology*; Oxford University Press: Oxford, UK, 2012.
49. Atlas, R.M.; Bartha, R. *Microbial Ecology, Fundamentals and Applications*, 3rd ed.; Benjamin/Cummings Publishing Co. Inc.: Redwood City, CA, USA, 1993.
50. Kertesz, M.A.; Frossard, E. Biological cycling of inorganic nutrients and metals in soils and their role in soil biogeochemistry. In *Soil Microbiology, Ecology, and Biochemistry*, 4th ed.; Parl, E.A., Ed.; Academic Press: San Diego, CA, USA, 2015.

51. Lovley, D.R. Microbial reduction of iron, manganese, and other metals. *Adv. Agron.* **1995**, *54*, 175–231.
52. Lovley, D.R. Electromicrobiology. *Annu. Rev. Microbiol.* **2012**, *66*, 391–409. [[CrossRef](#)]
53. Maier, R.M. Biogeochemical Cycling. In *Environmental Microbiology*, 2nd ed.; Maier, R.M., Pepper, I.L., Gerba, C.P., Eds.; Academic Press: San Diego, CA, USA, 2009.
54. Roden, E.E.; Wetzel, R.G. Organic carbon oxidation and suppression of methane production by microbial Fe(III) oxide reduction in vegetated and unvegetated freshwater wetland sediments. *Limnol. Oceanogr.* **1996**, *41*, 1733–1748. [[CrossRef](#)]
55. Lovley, D.R. Fe(II) and Mn(IV) reduction. In *Environmental Microbe–Metal Interactions*; Lovley, D.R., Ed.; ASM Press: Washington, DC, USA, 2000.
56. Woolfolk, C.A.; Whiteley, H.R. Reduction of inorganic compounds with molecular hydrogen by *Micrococcus lactilyticus*. *J. Bacteriol.* **1962**, *82*, 647–658. [[CrossRef](#)]
57. Roden, E.E.; Urrutia, M.M. Ferrous iron removal promotes microbial reduction of crystalline Iron(III) oxides. *Environ. Sci. Technol.* **1999**, *33*, 1847–1853. [[CrossRef](#)]
58. Paul, E.A.; Clark, F.E. *Soil Microbiology and Biochemistry*; Academic Press: San Diego, CA, USA, 1989.
59. Heron, G.; Crouzet, C.; Bourg, A.C.M.; Christenson, T.H. Speciation of Fe(II) and Fe(III) in contaminated aquifer sediments using chemical extraction techniques. *Environ. Sci. Technol.* **1994**, *28*, 1698–1705. [[CrossRef](#)]
60. Weber, K.A.; Achenbach, L.A.; Coates, J.D. Micro-organisms pumping iron: Anaerobic microbial iron oxidation and reduction. *Nat. Rev. Microbiol.* **2006**, *4*, 752–764. [[CrossRef](#)]
61. Roden, E.E.; Kappler, A.; Bauer, I.; Jiang, J.; Paul, A.; Stoesser, R.; Konishi, H.; Xu, H. Extracellular electron transfer through microbial reduction of solid-phase humic substances. *Nat. Geosci.* **2010**, *3*, 417–421. [[CrossRef](#)]
62. Nevin, K.P.; Lovley, D.R. Mechanisms for accessing insoluble Fe(III) oxide during dissimilatory Fe(III) reduction by *Geothrix fermentans*. *Appl. Environ. Microbiol.* **2002**, *68*, 2294–2299. [[CrossRef](#)]
63. Cotton, F.A.; Wilkinson, G. *Advanced Inorganic Chemistry*; John Wiley & Sons: New York, NY, USA, 1966.
64. Baes, C.F., Jr.; Mesmer, R.E. *The Hydrolysis of Cations*; John Wiley & Sons: New York, NY, USA, 1976.
65. Millero, F.J.; Sotolongo, S.; Izaguirre, M. The oxidation kinetics of Fe(II) in seawater. *Geochim. Cosmochim. Acta* **1987**, *51*, 793–801. [[CrossRef](#)]
66. Singer, P.C.; Stumm, W. The solubility of ferrous iron in carbonate-bearing waters. *J. Am. Water Works Assoc.* **1970**, *62*, 198–202. [[CrossRef](#)]
67. Stumm, W.; Lee, G.F. Oxygenation of ferrous iron. *Ind. Eng. Chem.* **1960**, *53*, 143–146. [[CrossRef](#)]
68. Wehrli, B. *Aquatic Chemical Kinetics*; Stumm, W., Ed.; Wiley-Interscience: New York, NY, USA, 1990; pp. 311–336.
69. Luther, G.W. The frontier-molecular-orbital theory approach in geochemical processes. In *Aquatic Chemical Kinetics*; Stumm, W., Ed.; Wiley-Interscience: New York, NY, USA, 1985; pp. 173–198.
70. King, D.W.; Lounsbury, H.A.; Millero, F.J. Rates and mechanism of Fe(II) oxidation at nanomolar total iron concentrations. *Environ. Sci. Technol.* **1995**, *29*, 818–824. [[CrossRef](#)]
71. Huang, J.; Jones, A.; Waite, T.D.; Chen, Y.; Huang, X.; Rosso, K.M.; Kappler, A.; Mansor, M.; Tratnyek, P.G.; Zhang, H. Fe(II) redox chemistry in the environment. *Chem. Rev.* **2021**, *121*, 8161–8233. [[CrossRef](#)]
72. Santana-Casiano, J.M.; Gonzalez-Davila, M.; Millero, F.J. Oxidation of nanomolar levels of Fe(II) with oxygen in natural waters. *Environ. Sci. Technol.* **2005**, *39*, 2073–2079. [[CrossRef](#)]
73. Neygens, E.; Baeyen, J. A review of classic Fenton’s peroxidation as an advanced oxidation technique. *J. Hazard. Mater.* **2003**, *B98*, 33–50. [[CrossRef](#)]
74. Leffler, A.J. A study of the hydrolysis of iron(III) ion by sodium bicarbonate using an inert NMR probe technique. *Inorg. Chem.* **1979**, *18*, 2529–2532. [[CrossRef](#)]
75. Hunt, J.P. *Metal Ions in Aqueous Solution*; W.A. Benjamin, Inc.: New York, NY, USA, 1965.
76. Flynn, C.M., Jr. Hydrolysis of inorganic iron(III) salts. *Chem. Rev.* **1984**, *84*, 31–41. [[CrossRef](#)]
77. Pass, G. *Ions in Solution (3) Inorganic Properties*; Clarendon Press: Oxford, UK, 1973.
78. Milburn, R.M.; Vosburgh, W.C. A spectrophotometric study of the hydrolysis of iron(III) ion. II. Polynuclear species. *J. Am. Chem. Soc.* **1955**, *77*, 1352–1355. [[CrossRef](#)]
79. Mulay, L.N.; Selwood, P.W. Hydrolysis of Fe³⁺: Magnetic and spectrophotometric studies on ferric perchlorate solutions. *J. Am. Chem. Soc.* **1955**, *77*, 2693–2701. [[CrossRef](#)]
80. Spiro, T.G.; Allerton, S.E.; Renner, J.; Terzis, A.; Bils, R.; Saltman, P. The hydrolytic polymerization of Fe(III). *J. Amer. Chem. Soc.* **1966**, *88*, 2721–2726. [[CrossRef](#)]
81. Sommer, R.A.; Margerum, D.W. Kinetic study of the hydroxoiron(III) dimer. *Inorg. Chem.* **1970**, *9*, 2517–2521.
82. Burgess, J. *Ions in Solution Basic Principles of Chemical Interactions*, 2nd ed.; Horwood Publishing: Chichester, UK, 1999.
83. Sparks, D.L. *Environmental Soil Chemistry*, 1st ed.; Academic Press: San Diego, CA, USA, 1995; p. 40.
84. Dixon, J.B.; Weed, S.B. (Eds.) *Minerals in Soil Environments*, 1st ed.; Soil Science Society of America: Madison, WI, USA, 1977.
85. Dixon, J.B.; Weed, S.B. (Eds.) *Minerals in Soil Environments*, 2nd ed.; Soil Science Society of America: Madison, WI, USA, 1989.
86. Harrison, A. *Fractals in Chemistry*; Oxford University Press: New York, NY, USA, 1995.

-
87. Schwertmann, U.; Taylor, R.M. Iron oxides. In *Minerals in Soil Environments*, 2nd ed.; Dixon, J.B., Weed, S.B., Eds.; Soil Science Society of America: Madison, WI, USA, 1989.
 88. Chukhrov, F.V.; Zvyagin, B.B.; Ermilova, L.P.; Gorshkov, A.I. New data on iron oxides in the weathering zone. *Proc. Int. Clay Conf.* 1972 **1973**, *1*, 397–404.

Disclaimer/Publisher’s Note: The statements, opinions and data contained in all publications are solely those of the individual author(s) and contributor(s) and not of MDPI and/or the editor(s). MDPI and/or the editor(s) disclaim responsibility for any injury to people or property resulting from any ideas, methods, instructions or products referred to in the content.